fMRI Analysis of Tremor in CIDP Patients

MSc Technical Medicine
Sophie van Bodegom

Amsterdam UMC
University Medical Centers

Universiteit Leiden
The Netherlands

TU Delft Delft University of Technology

Erasmus University Rotterdam

PAGE INTENTIONALLY LEFT BLANK

fMRI Analysis of tremor in CIDP Patients

Sophie van Bodegom

Student number : 4559231

02 June 2025

Thesis in partial fulfilment of the requirements for the joint degree of Master of Science in

Technical Medicine

Leiden University ; Delft University of Technology ; Erasmus University Rotterdam

Master thesis project (TM30004 ; 35 ECTSs)

Dept. of Biomechanical Engineering, TUDELFT

December 2024 – June 2025

Thesis committee members:

Dr. (MD PhD) Robert van den Berg, Erasmuc MC (chair)
Dr. (MD PhD) Fleur van Rootselaar, Amsterdam UMC
Dr. (MD PhD) Arthur Buijink, Amsterdam UMC
Dr. ir. Winfred Mugge, TU Delft

Universiteit Leiden

TU Delft Delft University of Technology

Erasmus Universiteit Rotterdam

PAGE INTENTIONALLY LEFT BLANK

Contents

List of Abbreviations

AUMC	Amsterdam University Medical Centers
BOLD	blood oxygen level-dependent
CIDP	chronic inflammatory demyelinating polyneuropathy
DBS	deep brain stimulation
DCM	dynamic causal model
EBCC	eyeblink classical conditioning
ECR	m. extensor carpi radialis
EFNS/PNS	European Federation of Neurological Societies and Peripheral Nerve Society
EMG	electromyography
FARM	Robust EMG-fMRI artifact reduction for motion
FCR	m. flexor carpi radialis
FDI	first m. interosseus dorsalis
fMRI	functional magnetic resonance imaging
FWE	family wise error
GLM	general linear model
MNI	Montreal Neurological Institute
MR	magnetic resonance
MRI	magnetic resonance imaging
ONLS	Overall Neuropathy Limitations Scale
TR	repetition time

Summary

Introduction

Upper limb tremor is a debilitating symptom of chronic inflammatory demyelinating polyneuropathy (CIDP). It generally does not respond well to therapy, and its pathophysiology is debated. Both a peripheral and central cause of tremor in CIDP have been hypothesized, and also an interplay between the two has been proposed. In case a central pathophysiology underlies tremor in CIDP patients, the cerebello-thalamo-cortical circuit may be involved. This has not been researched in CIDP before, but this circuit is known to play a role in other tremor disorders. Functional Magnetic Resonance Imaging (fMRI) can non-invasively assess brain activity, and will be used in this thesis to investigate a potential central pathophysiology of tremor in CIDP patients.

Aim

The aim of this thesis is to assess brain activity in the cerebello-thalamo-cortical circuit in CIDP patients who suffer from tremor, and compare this to the brain activity in this circuit in CIDP patients without tremor.

Methods

fMRI scans were acquired from both CIDP patients who suffered from tremor (tremor group), and CIDP patients without tremor (control group). All participants performed two motor tasks, alternated with rest. In the static motor task, they extended their arms in front of them, inducing a postural tremor in the patients from the tremor group. In the dynamic motor task, all participants extended their arms and additionally performed a tremorlike movement with their hands. In the tremor group, an intentional tremor cooccurred with the voluntary movement of the dynamic motor task. A general linear model was used to analyse the fMRI data. Within-group and between-group analyses of clusters of brain activity were performed using one-sample and two-sample t-tests respectively.

Results

9 tremulous CIDP patients and 12 controls were included in the analysis. In the between-group analysis of the static task, more activity in CIDP patients with tremor in comparison to CIDP patients without tremor was found in lobule VIII of the cerebellum, the premotor cortex and supplementary motor areas, the visual cortex, and the fusiform. In the dynamic task, CIDP patients with tremor showed more activity in lobules IV/V of the cerebellum, the premotor cortex and supplementary motor areas, the supramarginal gyrus, the pars orbitalis, the insula, and the Rolandic operculum.

Conclusion

The results suggest that there is more brain activity in the cerebello-thalamo-cortical circuit in CIDP patients who suffer from tremor in comparison to CIDP patients without tremor. However, the results of the dynamic task may be influenced by a difference in brain activity due to the voluntary tremorlike movement. Further research is necessary to first of all separate the brain activity related to tremor from activity resulting from the voluntary movement, and furthermore to give insight into if this hyperactivity in the cerebello-thalamo-cortical circuit in CIDP patients with tremor is the cause of tremor, maintaining it, or is a reflection of the tremor.

1 Introduction

1.1 CIDP

Chronic inflammatory demyelinating polyneuropathy (CIDP) is an immune-mediated type of acquired demyelinating neuropathy (6). The prevalence of CIDP ranges between 0.67 and 10.3 per 100,000 (7), with a predominance of elderly and male patients (7, 8). It is typically characterized by progressive or recurrent limb weakness that is symmetric and occurs both proximally and distally, sensory dysfunction, and is often accompanied by areflexia (9, 10). Additionally, CIDP can manifest in clinically atypical subtypes, which are defined according to the criteria of the European Federation of Neurological Societies and Peripheral Nerve Society (EFNS/PNS) (11). In the pathogenesis of CIDP, inflammation of the myelin sheaths of peripheral nerves cause segmental demyelination (Figure 1), which is followed by remyelination by Schwann cells. Despite this natural repair mechanism, nerve fibres are damaged and the accumulation of damage causes progressive neuropathy in patients.(8)

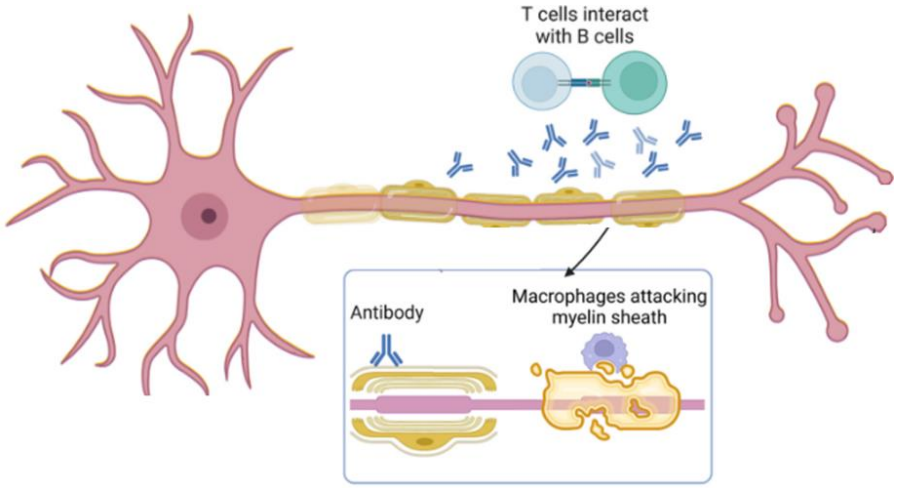

Figure 1: Pathogenesis of CIDP, adapted from Shastri et al.(4)

In addition to the muscle weakness and sensory dysfunction, CIDP patients can also suffer from tremor of the upper limbs. Tremor in neuropathy patients is often referred to as neuropathic tremor. This symptom is present in 45-83% of CIDP patients (12-15) and is associated with greater disability (Overall Neuropathy Limitations Scale (ONLS)) in comparison to CIDP patients without tremor (13). The reported frequency of the tremor in CIDP patients varies between 4-9Hz. The most prevailing activation condition of tremor in CIDP is postural, followed by an intentional tremor. However, rest tremor or a combination of these tremor types occur too (12, 14, 15).
CIDP is typically treated with immune-suppressive medication (16). In some patients, improvement in neuropathy is accompanied by a reduction of tremor (17, 18). However, the tremor in CIDP patients generally does not respond well to therapy (12).

1.2 Pathophysiology of Tremor in Neuropathy

The pathophysiology of tremor in CIDP, and more generally in neuropathy, is not fully understood. Different theories have been published, of which some point towards a peripheral cause of tremor, and others hypothesize the involvement of the central nervous system. Furthermore, an interplay between the two has been proposed. (12, 13, 15, 17, 19-38)

A factor that could help understand the aetiology of tremor, is whether there is a relation between the presence or severity of tremor, and the severity of the neuropathy symptoms. In case this relation exists, a peripheral cause is more likely. If, on the other hand, tremor severity and neuropathy severity seem to be unrelated, presumably the central nervous system is involved in the generation of tremor. In two studies by Dalakas et al. (17, 19), there seemed to be no relation between the development of tremor and the severity of neuropathy, proprioceptive loss, weakness or fatigue. However, the development of tremor might relate to disease activity (17). In another more recent study, a correlation between tremor severity and sensory deficits has been described (12). The relation between muscle strength and tremor has also been studied more recently. Some authors found that CIDP patients with muscle weakness were less likely to have a tremor (12, 13), whereas another did not find a relation between muscle strength and the presence of tremor (15).

Delayed peripheral nerve conduction is commonly discussed to be involved in neuropathic tremor. It has been suggested that mistimed peripheral inputs lead to abnormal central processing, resulting in tremor generation (20, 22-24). Prolonged peripheral motor responses (12, 13, 20, 22) and a delay in sensory afferent inputs (22) have been associated with the development of tremor. In another study, prolonged or absent motor and sensory responses correlated with tremor frequency (15). However, there are also studies that show no association between tremor and motor and sensory conduction velocity (13, 17, 25). Saifee et al. (13) found that although a decrease in conduction velocity did not predict the presence of tremor, a lower conduction velocity was correlated with tremor severity in neuropathy patients who had a tremor. Also conduction velocities of central pathways have been researched for abnormalities, but no evidence for a delay in these has been found analysing magnetic brain stimulation, somatosensory evoked potentials and stretch reflexes (22).

An observation potentially arguing in favour of a peripheral cause of tremor, is the fact that in some inflammatory neuropathy patients with tremor a higher tremor frequency is found in proximal muscles in comparison with more distal muscles (20). The reasoning is that peripheral inputs arising from proximal limb segments are likely to reach a central processor more quickly than inputs from the distal limb. Consequently, the input from proximal segments are provided more frequently than from distal limb segments, translating to a higher peak frequency proximally. Silsby et al.(15) found higher tremor frequencies proximally than distally in the limb that was affected by tremor, and in two other studies this phenomenon was observed in a part of the participants.
Another theory in which a tremor frequency gradient is involved exists too. Tremor in neuropathy has been proposed to be a mechanical tremor to which the stretch reflex mechanism contributes. For tremor resulting from a stretch reflex mechanism, tremor frequencies in proximal limb segments are lower than in the distal limb segments. As previously discussed, no gradient in this direction has been reported.(15) Furthermore, in a mechanical tremor you expect a frequency reduction by adding weight to the limb, which has not been reported (15, 20, 26).

Actually, the stability of the peak tremor frequencies as reported by multiple studies, implies the presence of a central generator or network (39). Besides the stable peak frequencies, there are more indications for central mechanisms of tremor generation. One area of interest is the cerebellum, as hyperactivity of the cerebellum in neuropathic tremor has been found in a previous functional magnetic resonance imaging (fMRI) study (21).
Schwingenschuh et al. (28) hypothesized that a central compensation mechanism exists to account for delays caused by the peripheral neuropathy, and that the cerebellum and its connections would be involved. To test this theory, they examined if patients with inflammatory neuropathies and tremor have evidence of dysfunction in the cerebellum and in the interactions with the sensorimotor cortex. The rates of eyeblink classical conditioning (EBCC) were used to investigate the cerebellum,

because if structural or functional impairments in the cerebellum exist, this leads to abnormalities in the EBCC (27, 29-31). In this study, an abnormally low EBCC was found in tremulous neuropathy patients compared to non-tremulous patients and healthy controls. In addition, their results suggested abnormal sensorimotor cortex plasticity. Another explanation for possible abnormalities of the cerebellum causing tremor involves neurofascin 155 antibodies. These antibodies are present in 7-15% of CIDP patients, and it has been suggested that these target the cerebellum.(32)
The effect of deep brain stimulation (DBS) on neuropathic tremor is another argument that there is a central influence on the tremor (33-37). In particular, stimulation of the ventral intermediate nucleus of the thalamus (12, 34, 38), and the posterior subthalamic area (40) has shown a significant reduction of neuropathic tremor.

1.3 Tremor Network

In case a central pathophysiology underlies tremor in CIDP patients, a tremor network may be involved. A tremor network is a group of interconnected brain regions that ensure that a tremor is generated and maintained. Although, as previously described, abnormalities in the cerebellum have been found (21, 28) and DBS in various locations has shown to effect neuropathic tremor (33-37), it has not previously been investigated whether a tremor network is active in neuropathic tremors. However, this has been examined in Parkinson's Disease associated tremor, essential tremor and dystonic tremor, and those results may provide starting points for researching a tremor network in CIDP.

EMG-fMRI studies have shown that resting tremor in Parkinson's Disease patients is associated with increased cerebral activity in the cerebello-thalamo-cortical circuit (41, 42). In healthy subjects, this circuit initiates and controls movements (43). It has been hypothesized that changes in the basal ganglia initiate tremor in Parkinson's Disease patients, after which oscillatory activity in the cerebello-thalamo-cortical circuit maintains the tremor (44).
Likewise to tremor in Parkinson's Disease, pathological oscillations within the cerebello-thalamo-cortical circuit are proposed to be involved in essential tremor (45). The origin of these oscillations is debated. It is hypothesized that the cerebellum itself is causing tremor by an increased drive, but also a functional disconnection of the dentate nucleus with (sub)cortical, and cerebellar areas have been thought to play a role in the pathophysiology of essential tremor.(46-48) Different subtypes exist among essential tremor patients, for example some have a resting tremor or subtle dystonia. Possibly a slightly different pathophysiology underlies the different presentations.(48)
Another type of tremor is dystonic tremor. The clinical presentation varies between different patients, and sometimes it clinically overlaps with essential tremor. In dystonic tremor, both the cerebellum and the basal ganglia are thought to be involved.(48, 49) Based on deep brain stimulation (DBS) studies, it has been hypothesized that more sinusoidal dystonic tremor is due to cerebellar alterations, whereas the basal ganglia might play a more prominent role in more jerky dystonic tremor (48, 50-52).

A neurological circuit which is involved in all of these tremor disorders, is the cerebello-thalamo-cortical circuit (Figure 2). Hence researching brain activity in this circuit in CIDP patients, is a relevant starting point for researching a potential central pathophysiology of tremor in CIDP patients.

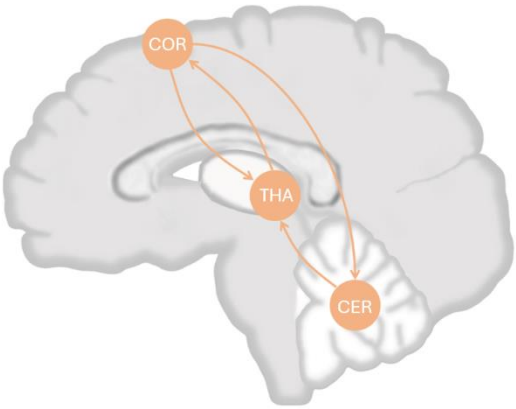

Figure 2: Cerebello-thalamo-cortical circuit, adapted from Zhong et al.(5)
COR: cortex, THA: thalamus; CER: cerebellum

1.4 EMG-fMRI

Functional Magnetic Resonance Imaging (fMRI) can be used to assess brain activity non-invasively. The most widely used technique in fMRI is to measure oxygen consumption of the brain, which indicates activity, based on blood oxygen level-dependent (BOLD) contrast.(53) fMRI studies can provide insight into the relation between movements and brain activity, if a motor task is performed by the subject during fMRI scanning. A common way to set-up such a study is using a block-design, in which blocks of motor task(s) are alternated with rest (54). In the analysis, the fMRI images acquired during a task block or rest block are evaluated separately, which enables comparison of brain activity between the different conditions. If additionally surface electromyography (EMG) is recorded simultaneously with fMRI acquisition (EMG-fMRI), this offers extra opportunities for the analysis. First of all, combined EMG-fMRI analysis allows to accurately determine the start and end of a task or rest block. Furthermore, it provides information on the execution of the task and additional muscle contractions of a subject at any moment within the EMG-fMRI acquisition.(54, 55) Overall, with simultaneous EMG-fMRI the relation between movement and brain activity can be studied in detail and more directly than with fMRI only, utilizing the high spatial resolution of fMRI imaging and high temporal resolution of EMG (53).

1.5 EMG-fMRI for Tremor Studies

A combined EMG-fMRI analysis is especially of added value when studying brain activity in tasks with a variance in execution, such as motor tasks in patients with tremor. A challenge is to distinguish between brain activations because of the performed motor task and simultaneous involuntary tremor movement (54). The study design can help to some extent with making this separation, for example by recording rest tremor in Parkinson's disease (21) patients when they are in rest, so theoretically no voluntary movement is involved in the measurement. Unfortunately, this experimental set-up leaves some opportunities for improvement, since there is also neuronal activity due to afferent sensory input present in tremor, which is not easily differentiated from brain activity resulting from tremor movement (56, 57). In case of a postural or action tremor, such as in essential tremor patients, it is even more complex to distinguish between brain activity related to voluntary movement and tremor, because they co-occur. However, earlier research has shown that amplitude variations in EMG data, after certain processing steps of the data have been performed, reflects extra EMG activity induced by the tremor (54, 58). When this EMG variable is used as a regressor in the EMG-fMRI analysis, the

relation between tremor-related EMG information and BOLD activity in the brain can be researched more reliably (55).

1.6 Thesis Aim & Hypothesis

1.6.1 Aim

For my thesis, EMG-fMRI data was used to investigate a potential central pathophysiology of tremor in CIDP patients, focussing on the cerebello-thalamo-cortical circuit. This was part of an ongoing PhD research on tremor in demyelinating neuropathies. Within the specific subgroup that was relevant for my thesis, seventeen measurements were already available and the fMRI data of some of the patients had been analysed. These analyses did not show significant differences between brain activity between CIDP patients with tremor and CIDP patients without tremor. My aim was to perform additional measurements to increase the sample size, and add the EMG data as a regressor to the general linear model (GLM) for the fMRI analysis. Both of these subgoals contributed to answering the following research question:

1.6.2 Research question

Is there more brain activity in the cerebello-thalamo-cortical circuit in CIDP patients who suffer from tremor in comparison to CIDP patients without tremor?

1.6.3 Hypothesis

My hypothesis was that there would be more brain activity in the cerebello-thalamo-cortical circuit in the tremor group compared to the control group. This was based on the rationale that the central nervous system is involved in tremor, more specifically a tremor network consisting of the cerebellum, thalamus and the motor cortex. I expected that the presence of tremor results in extra brain activity additional to activity related to voluntary movements, and to observe this in the brain areas of the cerebello-thalamo-cortical circuit.

2 Methods

2.1 Study Design

This study was performed at the departments of clinical neurophysiology and neurology of the Amsterdam University Medical Centers (AUMC), location Academic Medical Center. This project is a part of a larger study about tremor in demyelinating neuropathy, which was approved by the medical ethics committee AUMC, and conducted following the Declaration of Helsinki. All patients provided written informed consent before start of the study.

2.2 Study Population

Between 2018 and 2025, CIDP patients in the neurology out-patient clinic of the Amsterdam UMC were asked to participate in the study. Patients were eligible if they were ≥18 years old and physically able to perform motor tasks in the Magnetic Resonance Imaging (MRI) scanner. For the diagnosis of CIDP, the EFNS/PNS 2010 criteria (59) and/or EAN/PNS 2021 criteria (6) were used. In addition, patients fulfilling the clinical criteria and at least two supportive criteria were included.(9, 11) Patients were excluded if they had insufficient knowledge of the Dutch language, had contra-indications regarding MR safety, or a positive family history of tremor. There were two patient groups. In the tremor group, patients had a severe tremor or myoclonic tremor based on a tremor registration and questionnaires. Severe tremor was defined as either a score of ≥ 3 on the Archimedes Spirals or dot approximation task, a TETRAS subscale 4 score of ≥ 2.5, or limitations in activities of daily living. The tremor registration was performed around inclusion as part of standard clinical care, and consisted of recordings from the m. extensor carpi radialis (ECR), m. flexor carpi radialis (FCR), and first m. interosseus dorsalis (FDI) of both hands. During the registration, patients were measured in rest, with their arms extended in front of them, and this last task was repeated weight-loaded. If the EMG-fMRI measurement was performed substantially later in time than the inclusion, the tremor registration was repeated. At inclusion, participants filled out questionnaires on their tremor, disability, fatigue and pain. For the control group, CIDP patients without tremor, but who were eligible following the other criteria, were included. The groups were matched based on sex, age, and grip strength. Whenever a CIDP patient was included in the tremor group, another CIDP patients without tremor, but of the same sex and with comparable age and grip strength, was asked to participate. So the participants of both subgroups were matched 1:1.

2.3 Experimental Protocol

During the EMG-fMRI measurement, participants performed motor tasks with their upper limbs in the MRI scanner (Figure 3). Two different tasks were performed: a static motor task and a dynamic motor task. In the static task, participants were asked to extent their arms and hold them in the air for 20.3 s, alternated with a 20.3 s block of rest. These blocks were performed 12 times in one scanning run. During

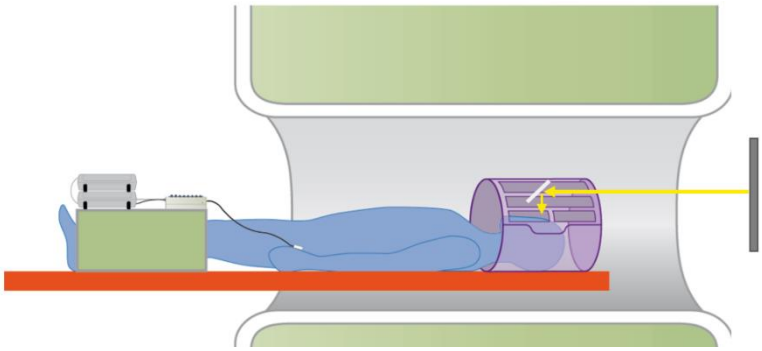

Figure 3: Participant in MRI scanner, with EMG equipment and visual cues, adapted from Warbrick & Stoermer (2)

the dynamic task, participants held their hands in a position similar to the static ask, but additionally made a tremor like movement with their hands at a frequency of 5-6Hz. This task was also performed twelve times, alternated with blocks of rest. During rest, arms were rested on the ulnar side of the hand along the side of the body or on the participant's lap, depending on how much space there was. Both tasks were repeated, adding up to a total of 4 scanning runs (dynamic, static, dynamic, static, see Figure 4). Instructions for what task to perform (made in Psychtoolbox (60), MATLAB version 2016b) were projected on a monitor that was visible from within the MRI scanner.

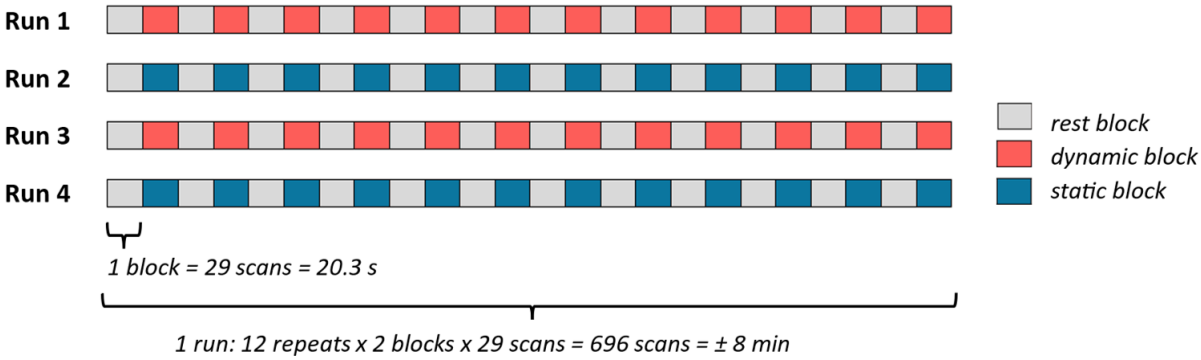

Figure 4: Experimental protocol

2.4 Data Acquisition

The data acquisition of the project was performed in 2019 - 2021, and in 2025 at the Spinoza Center for Neuroimaging in Amsterdam.

2.4.1 fMRI Recording

The MRI data was recorded using a 3T Achieva MRI scanner (Philips) with a 8 channel receive head coil. Functional T2*-weighted multi-shot EPI sequence (echo time 30ms; repetition time (TR) 700ms; flip angle 55°; field of view 216x216x130 mm; voxel size 2.7mm^3) were acquired. Forty-four axial slices were obtained for a total of 696 volumes. Additionally, high-resolution structural T1-weighted images were made (echo time 3.8ms; repetition time 9ms; flip angle 8°; voxel size 1 mm^3). Cushioning was added around the head to reduce movement, and next to the arms to prevent contact with the bore.

2.4.2 EMG Recording

Surface EMG was recorded with magnetic resonance (MR) -compatible surface electrodes from four muscles using bipolar electrodes: the FDI of both hands, and the ECR and FCR of the dominant arm, unless a tremor was only present of the other hand. In that case, the ECR and FCR were measured on the non-dominant arm. Additionally, ground electrodes were placed on both arms to improve the quality of the EMG signal. MR-compatible surface electrodes were connected to an MR-compatible EEG amplifier (BrainAmp, Brain Products GmbH, Germany) and a rechargeable battery to safely record EMG in the MRI-scanner. EMG was recorded with a sampling frequency of 5000 Hz, resolution of 0.1 µV, and digitally filtered with a low cutoff of 0.1 Hz, and a high cutoff of 1000 Hz.

2.5 Data Pre-processing

2.5.1 fMRI Pre-processing

Both functional and structural MRI data were pre-processed using MRIcron, Statistical Parametric Mapping software 12 (SPM12, Wellcome Trustcentre for Neuroimaging, London, UK) and MATLAB version 2023b. First, the structural scan and functional scans of the four runs were converted to NIFTI-files using MRIcron converter. Next, the data was visually inspected to check for unwanted distortions, excessive movement, and correct image orientation. Subsequently, multiple pre-processing steps, which are described below, were performed to reduce the effect of head movement, differences in anatomy, and equipment related artifacts on the fMRI data. These consisted of realignment, slice timing correction, co-registration, segmentation, normalisation, and smoothing of the data (Figure 5). After applying these steps, a cleaner bold signal analysis was possible. This pre-processing pipeline was applied to all runs of all participants.

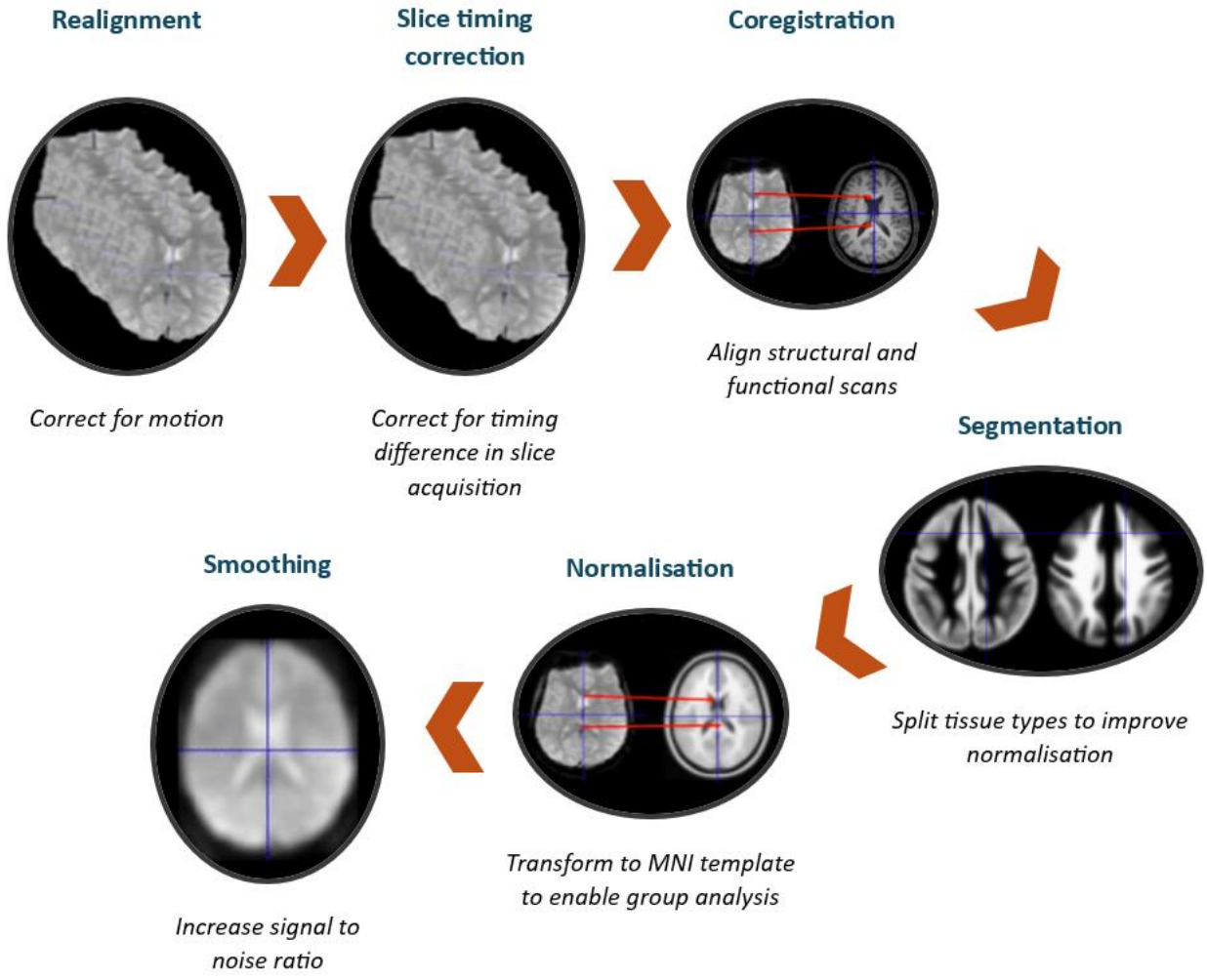

Figure 5: Pre-processing pipeline, adapted from Chang (1) and Jahn (3)

The first step of the pipeline was realignment of the functional data to account for head movement that occurred during scanning. SPM's *estimate and reslice* function was used, for which the full time series of runs were selected. A mean image was saved to be used in co-registration, and a text file with six movement parameters was saved to be used as regressors when fitting the GLM. The

movement parameters are the translation in the x, y, and z direction and the pitch, roll, and yaw rotation.
Secondly, slice timing correction was performed. Every volume of the fMRI scan consisted of forty-four slices which were obtained per four slices with bottom-up multi-slice scanning. As a result of this technique, there was a short delay between the acquisition of the first and last group of slices. To correct for the difference in timing, slice timing correction was performed on the realigned images. The applied settings were: number of slices: 44, TR: 0.7, slice order: [1:4:44 2:4:44 3:4:44 4:4:44], reference slice: 22.
During coregistration, for which the *coregister estimate* function was used, functional and structural data were aligned. The mean image generated in the realignment step was used as reference image, and the participant's anatomical scan as source image. The quality of the coregistration was checked by visually comparing the generated mean image and the anatomical scan, by checking the outline of the brain and ventricles.
Then, segmentation was applied to split the structural image into different tissue types (grey matter, white matter, cerebrospinal fluid, non-brain soft tissues, skull, and other) to improve normalization of the data in the next step. A forward deformation field containing coordinates of the different tissue types was saved to be used in normalization of the functional data.
Normalization of the data was performed to allow for group analyses using the write function. During normalisation, the data was transformed to fit the standard Montreal Neurological Institute (MNI) space. The deformation field created in the previous step was used together with the realigned and slice time corrected functional data. In the writing options, the voxel size was set at [3 3 3] to write the normalised images at a resolution close to the resolution at which they were acquired.
The final step of the procedure was to smooth the normalized data in order to increase the signal-to-noise ratio. This was achieved by averaging the signal in each voxel with a weighted average of the signal of neighbouring voxels. The size of the smoothing kernel was [6 6 6], following the rule of thumb to use a kernel double the voxel size.

2.5.2 EMG Pre-processing

The pre-processing of the EMG data consisted of two parts. First, the MR artifact was removed and, secondly, the EMG signal was further processed into a regressor that could be added to the GLM.

Removing MR artifact

The original plan was to use BrainVision Analyzer 2.2 software and its MR correction algorithm to remove the scanning artifact from the EMG data. However, when this algorithm was tweaked to the used scanning settings and applied to the data, the remaining EMG signal looked different than expected. There was still MR artifact left and tremor movement could not be distinguished clearly. After this scanning settings were examined, and it was concluded that the data had been acquired with multi-slice scanning instead of single-shot as assumed earlier. The shape of the MR artifact is a direct result of slice acquisition, which explained why the first attempt had not removed the scanning artifact sufficiently. Unfortunately, BrainVision Analyzer's MR correction algorithm is not able to process interleaved data. Therefore, it was decided to proceed with the Robust EMG-fMRI artifact reduction for motion (FARM) (61) algorithm, which is suitable for removing MR artifact from EMG data acquired during multi-slice fMRI scanning. See Appendix A for a more detailed explanation of why the FARM algorithm is suitable for the available EMG-fMRI data, and a basic explanation of how the FARM algorithm works.

EMG regressor

Getting acquainted with the code of the FARM algorithm and trying to make it run was more time consuming than hoped for (see Appendix A.3 for more explanation). Consequently, the step of creating a regressor from the EMG data was not reached within the time frame of this project. However, based on the literature study proceeding this thesis (see Appendix B) there was the following plan to construct the EMG regressor.

1) Select an EMG channel and a frequency band of interest for the analysis.
EMG was recorded from the first m. interosseus dorsalis of both hands, and the ECR and FCR muscle of one arm. From these, the channel with the best artifact correction and/or most clear tremor activity is selected.

2) Fourier transform the EMG data and extract a 5Hz band around the tremor frequency.
Either the peak tremor frequency from the tremor registration could be used for this, or preferably it could be determined from the EMG data recorded during the EMG-fMRI measurement itself.

3) Calculate the average power in the extracted frequency range per time segment of the EMG-fMRI recording and store all these values in a vector.
The length of each segment should be 0.7 s, which is identical to the TR of the fMRI scans, to ensure that there is a EMG value in the EMG vector for every fMRI scan.

4) Apply Gram-Schmidt orthogonalization with respect to the performed task (block), to make the EMG vectors independent of the performed task.

2.6 General Linear Model

2.6.1 Model Specification and First-Level Analysis

Prior to estimating the GLM, model specifications were defined. In the model, rest blocks were compared to task blocks, which both lasted 29 scans. In the data acquired in 2019-2021, there was a timing difference between the instruction of the participant to start with the first block, and obtaining the first scan. The MRI scanner had already made 18 volumes at the moment that the participant got the visual cue for their first task. This issue was corrected for in the model specifications, by adding 18 to all the onsets of the task blocks. The EMG data recorded simultaneously with fMRI scanning was used to determine if the onsets had to be corrected for a participant. Even prior to MR artifact correction, the blocks of rest and blocks of performing a task could be distinguished from each other in the EMG data. These EMG changes were compared to the scan triggers stored in the EMG data, and in this way it was concluded if the onsets had to be corrected. This analysis showed that the code controlling the scanner and the visual instructions had been updated prior to 2025. Therefore, the onsets did not have to be corrected in the newer set of data.
After the block design had been defined, the text file containing movement parameters (saved in the realignment step of fMRI pre-processing) were added to the model specification. When the model specification batch was run, this resulted in a design matrix.

Then the model was estimated based on the design matrix, and the contrast was defined for each run of every participant. In the contrast manager, new t-contrasts were defined for both the static and the dynamic tasks. They were specified as 1 (U>rest) and 1 (T>rest). The U>rest contrast was used to estimate the model for static tasks, during which the participants extended their arms in front of them. The T>rest contrast was applied to the dynamic task which asked the patients to make a

tremor like movement. The results of the model estimation and defined contrast were saved to be used in the group analyses.

2.6.2 Second-Level Analysis

In the second-level analysis, the results of the individual participants' first-level analysis were combined to perform a group-level analysis. The goal of this analysis is to examine a pattern of brain activity within a specific group, and subsequently compare brain activity between the tremor and control group. If participants of the tremor group did not have tremor on the day of the measurement, they were moved to the control group. One-sample t-tests were performed for four groups: static task tremor group, static task control group, dynamic task tremor group, and dynamic task control group.

Next, two-sample t-tests were used to compare the static task between the CIDP patients with and without tremor, and the dynamic task between both groups. The clusters of brain activity and their size (amount of voxels, k_E), intensity (T statistics), and Montreal Neurological Institute (MNI) coordinates were obtained. All t-tests were performed twice, first with a family wise error (FWE) corrected p-value < 0.05, and secondly with an uncorrected p-value < 0.001. In the analysis of uncorrected tests, only clusters ≥ 10 voxels were included.

3 Results

3.1 Patient Characteristics

At the end of February 2025, data had been collected from 23 patients. One patient was excluded post-hoc, because positive serum antibodies were found and this meant that this patient no longer had CIDP according to the criteria (9). Furthermore, the fMRI data of one participant was not available, leaving 21 participants for the analysis (Table 1). Nine patients with CIDP and tremor were included in the tremor group, and 12 CIDP patients without tremor in the control group. In the tremor group, there were relatively more male participants (tremor group: 67% vs. 58% in control group), and the average age and grip strength were slightly lower in comparison to the control group (age tremor group: 58.1 ± 15.2, age control group: 62.3 ± 7.7; grip strength tremor group (R/L): 71.8± 19.2 / 68.6 ± 16.0 kPa, grip strength control group (R/L): 78.1 ± 23.8 / 74.8 ± 21.7 kPa). In the tremor group, all patients suffered from action tremor. Most of them (7 out of 9) had both postural and intentional tremor, of whom two additionally suffered from a rest tremor. Two of the participants had solely a postural or intentional tremor. Only one patient used propranolol to suppress their tremor, the others did not use medication for this purpose.

Table 1: Patient Characteristics

	Tremor group (n=9)	**Control group (n=12)**
Sex [m/f]	6/3	7/5
Age [years ± sd]	58.1 ± 15.2	62.3 ± 7.7
Grip strength [kPa; R/L]	R: 71.8 ± 19.2 L: 68.6 ± 16.0	R: 78.1 ± 23.8 L: 74.8 ± 21.7
Disease duration [months ± sd]	105 ± 55.8	92.4 ± 52.1
Dominant hand [R/L]	7/2	12
Tremor characteristics		
Activation condition: *P & I & R* *P & I* *P* *I*	 2 5 1 1	-
-Tremor suppression medication [yes/no]	1/8	-

m: male; f: female; sd: standard deviation, R: right, L: left, P: postural, I: intentional, R: rest

3.2 Available Data

According to the measurement protocol, the goal was to record EMG-fMRI for two runs of both the static and dynamic task of all participants. For some participants, this was only partially realized due to insufficient scanning time at the Spinoza Centre, resulting in a limited number of recorded runs of them. In the tremor group, the entire protocol was scanned in five participants and partly in four, resulting in 14 scans of the static task and 15 of the dynamic task. In the control group, data from a complete scan protocol is available of nine patients and partly of three, resulting in 21 scans for both the static and dynamic task. Corresponding EMG data was available for the majority of these fMRI scans, but the EMG of one participant from the control group seems to be missing. See Appendix C for an overview of the available data per participant.

The model estimation of the second run of the dynamic motor task in one of the control patients, resulted in an error because the length of the regressor with the movement parameters was not

commensurate with the data point of the pre-processed fMRI scan. The error was not resolved, and therefore this run of the participant was not included in the analysis of the dynamic motor task.

3.3 Static Motor Task

3.3.1 Static Motor Task within Tremor Group

The one-sample t-test of the tremor group during the static task compared to rest did not show any brain activity at a FWE-corrected p-value < 0.05, but the uncorrected test with p < 0.001 showed fourteen clusters of activity (Figure 6), of which four consisted of more than ten voxels (Table 2). These were located in the right and left premotor cortex and supplementary motor areas, and the left supramarginal gyrus. See Appendix D.1.1 for a more extensive table with statistics of all identified clusters.

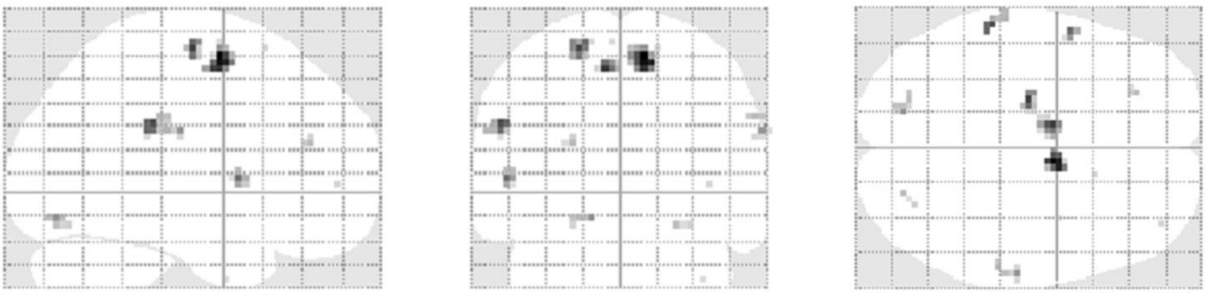

Figure 6: Sagittal, coronal and transverse view of brain activity during static motor task in tremor group (p<0.001 uncorrected)

Table 2: Statistics of static motor task in tremor group (p<0.001 uncorrected)

Cluster-level		Peak-level		MNI coordinates			Area
k_E	p	T	p	X	Y	Z	
32	0.023	6.23	0.000	9	-4	59	Right premotor cortex + supplementary motor area
19	0.069	5.56	0.000	-9	-4	53	Left premotor cortex + supplementary motor area
17	0.084	5.40	0.000	-21	-16	62	Left premotor cortex + supplementary motor area
14	0.113	5.35	0.000	-57	-34	29	Left supramarginal gyrus

k_E: amount of voxels, p: p-value; T: T-statistic

3.3.2 Static Motor Task within Control Group

Likewise to the tremor group, no brain activity was detected with a one-sample t-test with FWE-corrected p-value < 0.05 in the control group of the static task versus rest. When analysing the results at a significance level of $p_{uncorrected} < 0.001$ (see also Appendix D.1.2), activity was found in the left visual cortex, the vermis of the cerebellum, frontal white matter, and lobules IV/V of the right cerebellum (Figure 7, Table 3). Only the cluster in the left visual cortex was larger than ten voxels (18 voxels, p = 0.181) and this cluster had a peak intensity of 5.23 (p = 0.000). See Appendix D.1.2 for statistics of the smaller clusters.

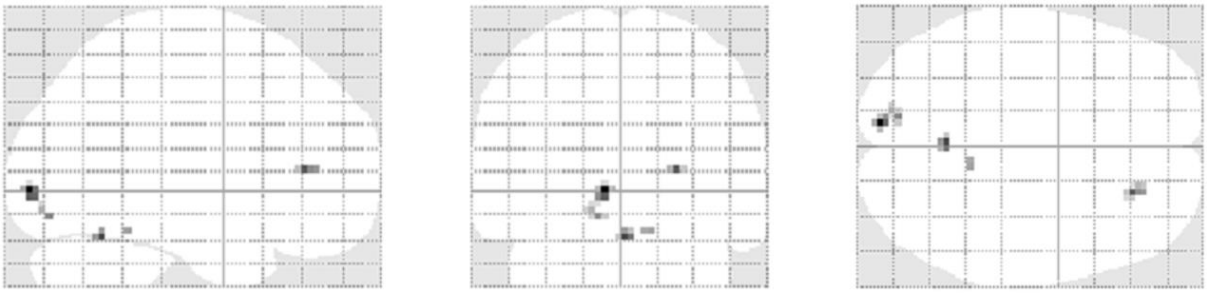

Figure 7: Sagittal, coronal and transverse view of brain activity during static motor task in control group (p<0.001 uncorrected)

Table 3: Statistics of static motor task in control group (p<0.001 uncorrected)

Cluster-level		Peak-level		MNI coordinates			Area
k_E	p	T	p	X	Y	Z	
18	0.181	5.23	0.000	-9	-91	-1	Left visual cortex

k_E: amount of voxels, p: p-value; T: T-statistic

3.3.3 Comparison Tremor and Control Group Static Motor Task

The two sample t-test comparing brain activity between the tremor and control group while performing the static task, showed two statistically significant clusters with a FWE-corrected p-value < 0.05 (Figure 8). The location of the two clusters corresponded to the right and left premotor cortex and supplementary motor areas. The right cluster had a size of 3 voxels ($p_{FWE\text{-}corrected}$ = 0.012) with a peak intensity of 5.52 ($p_{FWE\text{-}corr}$ = 0.042), and the cluster on the left had a size of 1 voxel ($p_{FWE\text{-}corrected}$ = 0.025) and a peak intensity of 5.5 ($p_{FWE\text{-}corrected}$ = 0.044) (Table 4).

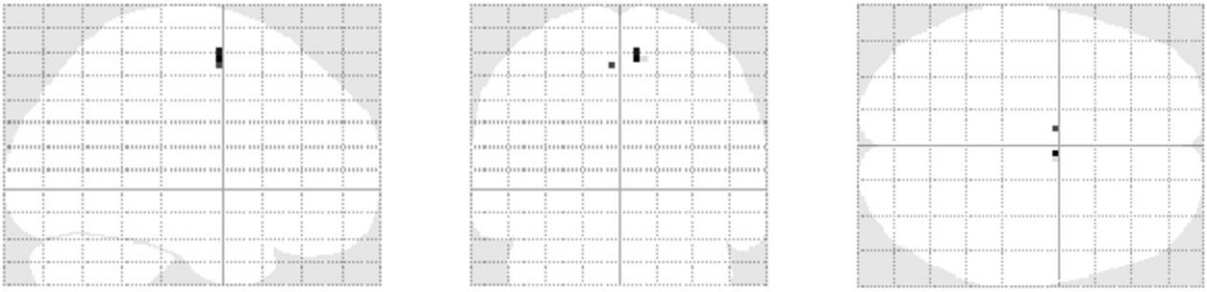

Figure 8: Sagittal, coronal and transverse view of brain activity during static motor task in tremor group in comparison to control group (FWE-corrected p<0.05)

Table 4: Statistics of comparison tremor and control group for static motor task (FWE-corrected p<0.05)

Cluster-level		Peak-level		MNI coordinates			Area
k_E	$p_{FWE\text{-}corr}$	T	$p_{FWE\text{-}corr}$	X	Y	Z	
3	0.012	5.52	0.042	6	-4	56	Right premotor cortex + supplementary motor area
1	0.025	5.50	0.044	-6	-4	53	Left premotor cortex supplementary motor area

k_E: amount of voxels, $p_{FWE\text{-}corr}$: FWE-corrected p-value; T: T-statistic

When the tremor and control group are compared with uncorrected testing, this showed twenty-two clusters of more activity in the tremor group in comparison to the control group (Figure 9, Appendix D.1.3). Eight of them were larger than or equal to ten voxels. The two largest clusters were located in the right premotor cortex and supplementary motor area which had a size of 52 voxels (p=0.027) and 41 voxels (p = 0.045) and a peak intensity of 4.61 (p = 0.000) and 4.35 (p = 0.000) respectively. The other clusters with a size ≥ 10 voxels were located in lobule IIX of the right cerebellum, right fusiform, gyrus lingualis of the left visual cortex, and one cluster was found outside of in atlas defined areas (Table 5).

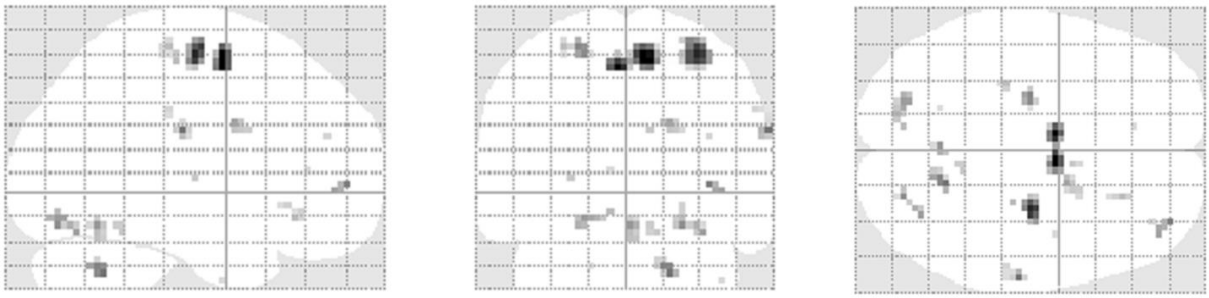

Figure 9: Sagittal, coronal and transverse view of brain activity during static motor task in tremor group in comparison to control group (p<0.001 uncorrected)

Table 5: Statistics of comparison tremor and control group for static motor task (p<0.001 uncorrected)

Cluster-level		Peak-level		MNI coordinates			Area
k_E	p	T	p	X	Y	Z	
52	0.027	4.61	0.000	6	-4	56	Right premotor cortex + supplementary motor area
41	0.045	4.35	0.000	30	-16	59	Right premotor cortex + supplementary motor area
12	0.256	3.86	0.000	18	-58	-37	Right cerebellum lobule VIII
13	0.237	3.72	0.000	-24	-16	62	Left premotor cortex + supplementary motor area
10	0.299	3.66	0.000	24	-79	-16	Right visual association area
12	0.256	3.59	0.000	0	-61	-16	Right fusiform
12	0.256	3.58	0.000	-21	-79	-13	Gyrus lingualis of visual cortex left
12	0.256	3.51	0.000	18	2	29	Outside defined area

k_E: amount of voxels, p: p-value; T: T-statistic

3.4 Dynamic Motor Task

3.4.1 Dynamic Motor Task within Tremor Group

The one-sample t-test of the dynamic task versus rest of the tremor group did not show any brain activity with a FWE-corrected p-value < 0.05. When the test was repeated with an uncorrected p-value < 0.001, forty clusters were found of which ten were larger than 10 voxels (Figure 10, Table 6, Appendix D.2.1). The three clusters with the highest intensity were located in the left putamen (size: 11 voxels (p = 0.196); peak-intensity: 7.47 (p = 0.000)), right premotor cortex and supplementary

motor area (size: 385 voxels (p = 0.000); peak-intensity: 7.40 (p = 0.000)), and left visual cortex (size: 399 voxels (p = 0.000); peak-intensity: 6.64 (p = 0.000)). See Table 6 for the statistics of these clusters.

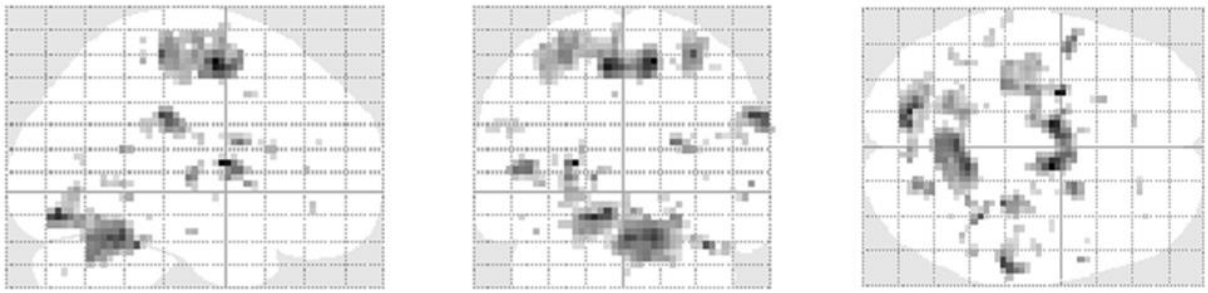

Figure 10: Sagittal, coronal and transverse view of brain activity during dynamic motor task in tremor group (p<0.001 uncorrected)

Table 6: Statistics of dynamic motor task in tremor group (p<0.001 uncorrected)

Cluster-level		**Peak-level**		**MNI coordinates**			**Area**
k_E	**p**	**T**	**p**	**X**	**Y**	**Z**	
11	0.196	7.47	0.000	-24	-4	11	Left putamen
385	0.000	7.40	0.000	12	-7	56	Right premotor cortex + supplementary motor area
399	0.000	6.64	0.000	-15	-79	-13	Left visual cortex
55	0.009	6.26	0.000	60	-31	32	Right supramarginal gyrus
67	0.004	6.01	0.000	30	-31	59	Right primary sensory cortex
15	0.135	5.99	0.000	36	-43	-25	Right cerebellum lobule VI
23	0.070	5.58	0.000	-51	5	8	Left premotor cortex + supplementary motor area
16	0.124	5.50	0.000	21	5	20	Outside defined area
12	0.178	5.39	0.000	-27	-19	5	Outside defined area
21	0.082	5.21	0.000	21	-76	-13	Right visual cortex

k_E: amount of voxels, p: p-value; T: T-statistic

3.4.2 Dynamic Motor Task within Control Group

In the control group, the one-sample t-test performed on scans acquired during the dynamic task versus rest, did find two statistically significant clusters at a FWE-corrected p-value < 0.05 (Figure 11). The first is located in the third lobule of the right cerebellum and has a size of 24 voxels ($p_{FWE\text{-}corr:}$= 0.000) and a peak intensity of 6.72 ($p_{FWE\text{-}corr:}$= 0.020) (Table 7). The second identified cluster was only 2 voxels in size ($p_{FWE\text{-}corr:}$ = 0.017), had a peak intensity of 6.22 ($p_{FWE\text{-}corr:}$ = 0.046), and was located in the left primary motor cortex.

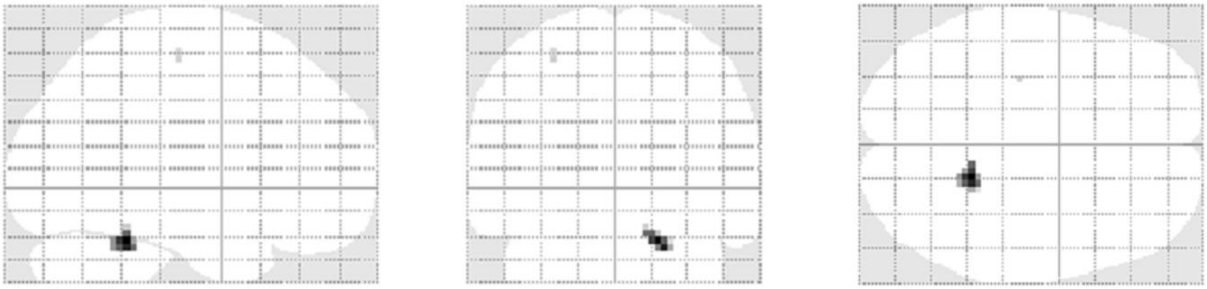

Figure 11: Sagittal, coronal and transverse view of brain activity during dynamic motor task in control group (FWE-corrected p<0.05)

Table 7: Statistics of dynamic motor task in control group (FWE-corrected p<0.05)

Cluster-level		Peak-level		MNI coordinates			Area
k_E	$p_{FWE-corr}$	T	$p_{FWE-corr}$	X	Y	Z	
24	0.000	6.72	0.020	18	-46	-25	Right cerebellum lobule III
2	0.017	6.22	0.046	-30	-22	56	Left primary motor cortex

k_E: amount of voxels, $p_{FWE-corr}$: FWE-corrected p-value; T: T-statistic

The two-sample t-test with an uncorrected p-value < 0.001, identified eight clusters ≥ 10 voxels (twenty-eight clusters in total) (Figure 12, Appendix D.2.2). The largest clusters were located in lobule III of the right cerebellum (size: 973 voxels (p = 0.000); peak-intensity: 6.72 (p = 0.000)) and the left primary motor cortex (size: 618 voxels (p = 0.000); peak-intensity: 6.22 (p = 0.000)), and the others were found in lobule VIII of the left cerebellum, lobule IX of the right cerebellum, left and right Rolandic operculum, and right supramarginal gyrus. One cluster was located outside in atlases defined areas. See Table 8 for the statistics.

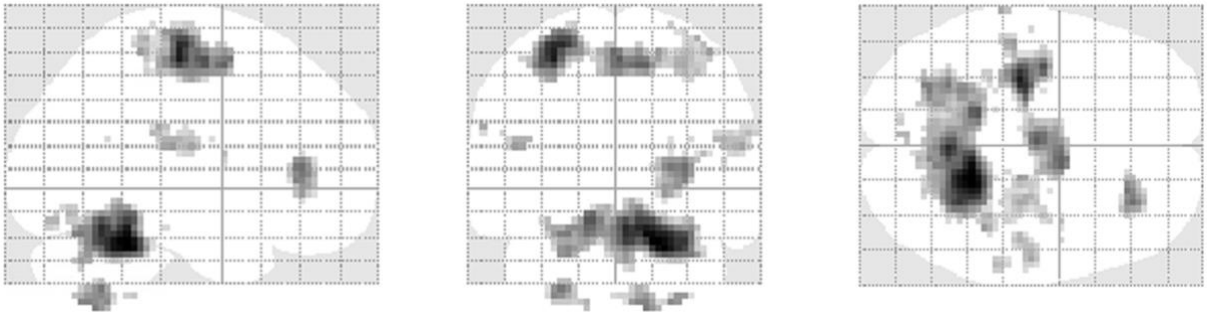

Figure 12: Sagittal, coronal and transverse view of brain activity during dynamic motor task in control group (p<0.001 uncorrected)

Table 8: Statistics of dynamic motor task in control group (p<0.001 uncorrected)

Cluster-level		Peak-level		MNI coordinates			Area
k_E	p	T	p	X	Y	Z	
973	0.000	6.72	0.000	18	-46	-25	Right cerebellum lobule III
618	0.000	6.22	0.000	-30	-22	56	Left primary motor cortex
102	0.008	5.10	0.000	30	35	8	Outside defined area
55	0.041	4.95	0.000	-27	-58	-46	Left cerebellum lobule VIII
51	0.048	4.88	0.000	12	-61	-55	Right cerebellum lobule IX
18	0.220	4.46	0.000	-48	-25	17	Left Rolandic operculum
47	0.056	4.33	0.000	57	-16	17	Right Rolandic operculum
10	0.359	4.07	0.000	60	-34	23	Right supramarginal gyrus

k_E: amount of voxels, p: p-value; T: T-statistic

3.4.3 Comparison Tremor and Control Group Dynamic Motor Task

Performing a two-sample t-test to compare brain activity between the test and control group during the dynamic task, resulted in six clusters with FWE-corrected p-value < 0.05 (Figure 13) which were located in the right cerebellum, and left premotor cortex, supplementary motor areas, and primary motor cortex. Of these, the cluster in the right cerebellum was the largest. It consisted of 26 voxels ($p_{FWE\text{-}corrected}$ = 0.00) and had a peak intensity of 6.60 ($p_{FWE\text{-}corrected}$ = 0.002). See Table 9 for all statistics.

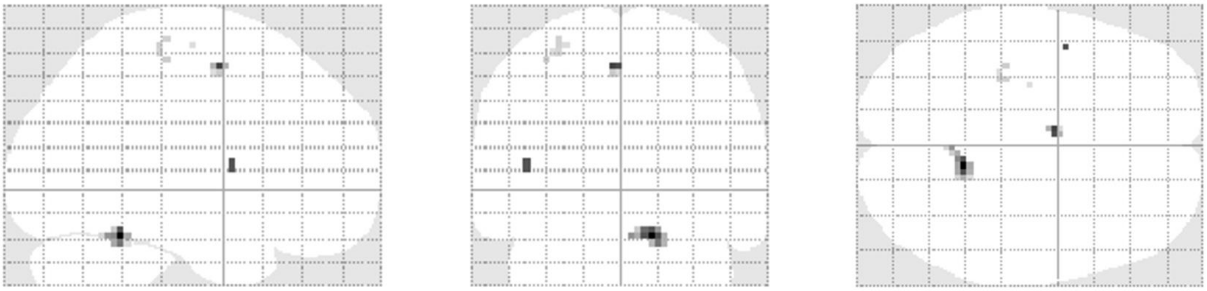

Figure 13: Sagittal, coronal and transverse view of brain activity during dynamic motor task in tremor group in comparison to control group (FWE-corrected p<0.05)

Table 9: Statistics of comparison tremor and control group for dynamic motor task (FWE-corrected p<0.05)

Cluster-level		Peak-level		MNI coordinates			Area
k_E	$p_{FWE\text{-}corr}$	T	$p_{FWE\text{-}corr}$	X	Y	Z	
26	0.000	6.60	0.002	12	-49	-22	Right cerebellum lobule IV/V
8	0.005	6.20	0.006	-6	-4	53	Left premotor cortex + supplementary motor area
2	0.020	6.12	0.008	-45	2	8	Left insula
1	0.028	5.46	0.038	-36	-28	56	Left primary motor cortex
4	0.011	5.44	0.040	-30	-28	65	Left primary motor cortex
1	0.028	5.38	0.047	-27	-16	62	Left premotor cortex + supplementary motor area

k_E: amount of voxels, $p_{FWE\text{-}corr}$: FWE-corrected p-value; T: T-statistic

Additional to the two-sample t-test with a FWE-corrected p-value < 0.05, the test was performed with an uncorrected p-value < 0.001. This analysis identified thirty-six clusters of which ten were ≥ 10 voxels (Figure 14, Table 10, Appendix D.2.3). The cluster were located in lobule IV/V of the right cerebellum, left premotor cortex and supplementary motor area, left insula, right and left supramarginal gyrus, right primary motor cortex, right pars orbitalis, left Rolandic operculum, and two outside of an in atlases defined area.

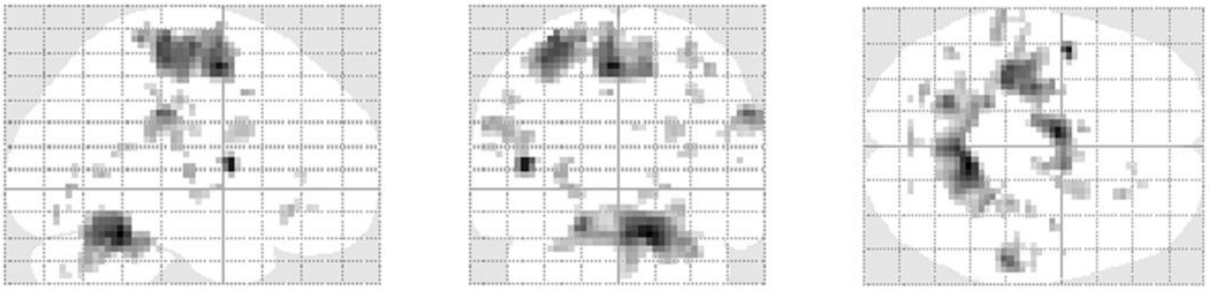

Figure 14: Sagittal, coronal and transverse view of brain activity during dynamic motor task in tremor group in comparison to control group (p<0.001 uncorrected)

Table 10: Statistics of comparison tremor and control group for dynamic motor task (p<0.001 uncorrected)

Cluster-level		Peak-level		MNI coordinates			Area
k_E	p	T	p	X	Y	Z	
526	0.000	6.60	0.000	12	-49	-22	Right cerebellum lobule IV/V
553	0.000	6.20	0.000	-6	-4	53	Left premotor cortex + supplementary motor area
24	0.144	6.12	0.000	-45	2	8	Left insula
68	0.021	5.13	0.000	57	-31	32	Right supramarginal gyrus
40	0.066	4.17	0.000	-63	-31	26	Left supramarginal gyrus
15	0.243	4.17	0.000	30	-28	59	Right primary motor cortex
13	0.276	4.02	0.000	27	29	-10	Right pars orbitalis
11	0.316	4.01	0.000	0	-79	-13	Outside defined area
17	0.215	3.60	0.000	-45	-25	20	Left Rolandic operculum
34	0.087	3.84	0.000	24	8	26	Outside defined area

k_E: amount of voxels, p: p-value; T: T-statistic

3.5 Overview of Results

In Table 11, an overview is shown of the locations of detected clusters of brain activity in all within-group and between-group analyses.

Table 11: Overview of identified clusters in second-level-analysis

Area	Static motor task			Dynamic motor task		
	Tremor	**Control**	**Comparison**	**Tremor**	**Control**	**Comparison**
Cerebellum						
Lobule III					R*	
Lobule IV/V					R	R*
Lobule VI				R		
Lobule VIII			R			
Lobule IX					R	
Vermis						
Cortex						
PMC + SMA	R L		R* L*	R L		L*
MC1					L*	R L*
SC1				R		
SMG	L			R	R	R L
Visual Cortex		L	L	R L		
VAC			R			
Pars orbitalis						R
Insula						L*
Rolandic Op.					R L	L
Fusiform			R			
Basal ganglia						
Putamen				L		

*PMC: premotor cortex; SMA: supplementary motor area; MC1: primary motor cortex; SC1: Primary sensory cortex; SMG: supramarginal gyrus; VAC: visual association cortex Rolandic Op.: Rolandic operculum; R: cluster detected in right hemisphere; L: cluster detected in left hemisphere; *also detected at* $p_{FWE\text{-}corrected} < 0.05$

4 Discussion

The aim of my thesis was to investigate a potential central pathophysiology of tremor in CIDP patients, and more specifically if there is more brain activity in the cerebello-thalamo-cortical circuit in CIDP patients who suffer from tremor in comparison to CIDP patients without tremor.

4.1 Motor Task Results

During the static motor task, participants were asked to extend their arms in front of them for approximately 20 s, alternated with rest. This task was designed to induce a postural tremor in the patients suffering from tremor, while in the control group theoretically no movement was present when executing the static motor task. This set-up allowed for an analysis of the brain activity related to tremor activity, and a comparison between tremulous and non-tremulous CIDP patients. In the dynamic motor task, participants from both groups performed movements in the task blocks. They all performed a tremorlike movement with the hands, and in the tremor group this voluntary movement was accompanied by tremor activity from intentional tremor induced in this task. Originally, the plan was to separate the brain activity from the voluntary tremorlike movement and the activity resulting from involuntary tremor by orthogonalizing the EMG data. Since this processing of the EMG data was not achieved, the total brain activity of the two subgroups were analysed and compared.

4.1.1 Static Motor Task

The within-group analyses of the static task showed a couple clusters ≥ 10 voxels of brain activity in the tremor group, and one cluster ≥ 10 voxels in the control group when the one-sample t-test were performed without FWE-correction and a p-value < 0.001. The clusters in the tremor group were located in the premotor cortex and supplementary motor area, and one in the left supramarginal gyrus. In contrast, no clusters of brain activity in motor related areas were identified in the control group, but one cluster was found in the left visual cortex. This activity in the visual cortex might be due to the participants focussing on the visual cues to perform either the task or rest block. However, this seems to be just as relevant during the rest blocks. This notion weakens the preceding explanation, since the contrasts used in the one-sample t-test are based on the task vs. rest block. As a results, only differences between both blocks are shown in the analyses.

When a two-sample t-test (uncorrected p-value < 0.001) was performed to analyse the brain activity of the tremor group in comparison to the control group, a difference in activity in the motor cortex was apparent. A cluster ≥ 10 voxels was seen in both the right and left premotor cortex and supplementary motor area. In addition to extra activity in these motor areas, also a cluster ≥ 10 voxels of higher brain activity in lobule VIII of the right cerebellum was detected. Furthermore, smaller clusters in lobules IV/V and the vermis of the cerebellum were seen. Sensorimotor areas of the brain project to lobules IV-VI and VIII, and in a meta-analysis of functional imaging studies of cerebellar activation patterns it was apparent that sensorimotor tasks activated the anterior lobe and lobule VIII of the cerebellum (62). In another study, hand movement engaged lobules V and VIII of the cerebellum (63). In both of these studies, participants performed voluntary movement whereas in the static motor task of this research, the tremor group performed an involuntary tremor movement. The similarities in results, could arise from a comparable underlying circuit. Other areas in which clusters ≥ 10 voxels were seen in the between group analysis, were the left visual cortex, right visual association area, and the right fusiform. The cluster in the left visual cortex is striking, because in the within-group analyses a cluster was identified in the control group and not the tremor group. However, the exact location of the cluster found in the within-analysis of the control group and the

cluster in the between-analysis are different, which could explain this finding. The activity in the fusiform could be grouped together with the clusters in the visual cortex areas, via its function in reading (64). No indication of differences in thalamus activity between the two subgroups were found in the analysis.

4.1.2 Dynamic Motor Task

Similar to the within tremor group analysis of the static task, the within tremor group analysis of the dynamic motor task (uncorrected p-value < 0.001) showed clusters of which some were located in areas of the cortex related to motor activity (right and left premotor cortex and supplementary motor area, right supramarginal gyrus), and in the visual cortex. Furthermore, clusters of brain activity were found in the right primary sensory cortex, lobule VI of the right cerebellum, and the left putamen. The cluster in the primary sensory cortex is located in the area that processes afferent inputs from the upper limb. Lobule VI of the cerebellum is engaged in more cognitively demanding tasks (62), but has also been linked to coordination (65). The left putamen is involved in motor control too, via connections with the primary motor cortex and supplementary motor area (66, 67).
In the control group, clusters ≥ 10 voxels with uncorrected p-value < 0.001 were found in the supramarginal gyrus, lobules III, IV/V, and IX of the cerebellum, the left primary motor cortex, and the Rolandic operculum. Both lobule III and IV/V are involved in coordinating motor tasks, and activity in the Rolandic operculum during a motor task has been found before in motor tasks (62). The cluster in the left primary motor cortex was located in an area that corresponds to the right arm.
In the dynamic tasks, when all participants performed voluntary movements, this was reflected in clusters of brain activity in areas related to sensorimotor processing and motor control in the within-group analyses of both the tremor and control group.

When the tremor and control group were compared with a two-sample t-test with an uncorrected p-value < 0.001, clusters ≥ 10 voxels of more activity in the tremor group compared to the control group were detected in the left premotor cortex and supplementary motor area, right and left supramarginal gyrus, lobules IV/V of the right cerebellum, the left Rolandic operculum, the left insula, and the right pars orbitalis. Whereas the insula is involved in sensorimotor processing (68) similar to most of the other detected clusters, the pars orbitalis is associated with abstract cognitive functions (69) and therefore a cluster in this area was not expected.
The dynamic task was set-up to induce an intentional tremor in the tremor group, additional to the movement related to the voluntary movement which was present in both subgroups. Possibly, the clusters identified in the between-group analysis reflect brain activity related to the tremor. However, in the current fMRI analysis, it can not be stated that the amount of brain activity due to the voluntary movement was similar between both groups, hence it is difficult to interpret the results related to tremor activity.

4.1.3 Cerebello-Thalamo-Cortical Circuit

So in both the static and dynamic task, additional brain activity was found in the tremor group compared to the control group in to motor related areas of the cortex and cerebellum, which is partly in line with the hypothesis that there is more brain activation in the cerebello-thalamo-cortical circuit in tremulous CIDP patients compared to non-tremulous CIDP patients. No proof of activity in the thalamus was found in this research. Based on its function in motor control (70), activity in the thalamus was expected in the participants, especially since clusters in the cortex and cerebellum to which the thalamus is connected did show motor activity. In other tremor studies in essential tremor and Parkinson's disease patients, EMG-fMRI analyses did detect clusters of brain activity in nodes of the thalamus. Additional to the clusters in the thalamus, they also detected clusters of brain activity

in the (pre)motor cortex, supplementary motor areas and lobules of the cerebellum, which is similar to the results of this research.(55, 57, 71, 72)

4.2 Methodological choices

In my thesis, multiple choices were made in both pre-processing of the fMRI data and performing the analyses, which may have influenced the results.

4.2.1 Pre-processing fMRI

Numerous pre-processing are required to prepare fMRI data for a statistical analysis (73). In this research, motion correction via realignment, slice timing correction, coregistration of the anatomical and functional scans, segmentation, normalisation, and smoothing were performed. All of these steps, except for segmentation, involve averaging or moving voxels of the fMRI scans to correct for spatial and temporal differences between scans and subjects. Although these corrections are performed to enable the analysis of the BOLD-signal, there is also a risk of impairing the data.
In this research, realignment was performed first, followed by slice timing correction. Slice timing correction was incorporated in the pre-processing pipeline, to correct for temporally misalignment between fMRI slices (73), even though the scans were acquired with a TR of 0.7 s. Slice timing correction is not advised in sub-second TR data (74), because it is assumed that the data will not benefit from it. This is based on the assumption that the BOLD signal is slow, and so any signal change due to temporal offsets is likely to also be small. However, the GLM is extremely sensitive to small shifts in signals, so possibly fMRI data acquired with a short TR does benefit from slice timing correction.(73) Parker et al. (73) tested slice timing correction in data sets which were acquired and pre-processed with different settings, to examine the benefit of slice timing correction related to other pre-processing steps. They found that applying both slice timing correction and realignment in any order is beneficial, also in sub-second TRs, although the effect is smaller when a larger smoothing kernel is applied. An alternative for slice timing correction which has been proposed for shorter TRs (74) is to use temporal derivatives. This might be worth looking into for future research.

In the current project, slice timing correction was performed after motor correction via realignment, as this seemed the most commonly applied order among tutorials (75, 76) and no consensus on the order of the different pre-processing steps exists (even though it has shown to influence the results of the fMRI analysis) (77, 78). However, one tutorial advises to use slice timing correction first if you have interleaved data or expect significant head movement (74). Head movement in this study was minimized by adding cushioning around the head while scanning, but it was limited to an acceptable extent. Hindsight, starting with slice timing correction and then performing realignment of the data might have been a better order in this research.

In the coregistration of the pre-processing pipeline, SPMs software aligned the anatomical and functional data, which was later warped to a standard MNI template during normalisation. An extra step that could have been performed in coregistration, is to manually set the origin to the anterior commissure in the structural data. The reason to place the origin in the anterior commissure, is that the in normalisation used MNI template has this as their origin. This was not performed and although results were visually checked for major misalignment, setting the origin manually could have improved the pre-processing of the fMRI data.

4.2.2 General Linear Model and Statistical Analysis

In addition to correcting for the timing difference between the start of the fMRI scans and the visual cues in the data collected in 2019-2021, another adjustment of the onsets in the model specifications

was considered. It was contemplated to not include the first few scans of each task and rest block, because there is a delay in the participant's response to the cue to switch blocks. As a result, the patient does not perform the given task at the start of a block yet. However, SPM already takes a transition time between blocks into account, so the plan to adjust this myself was put aside.

The GLM was used for a whole-brain analysis, instead of using a mask to focus on regions of interest, even though there was a hypothesis of the involvement of the cerebello-thalamo-corctical circuit. There are a couple of reasons to apply a mask in the analysis. One of them being that a reduction in the amount of data to be analysed, results in a computationally less demanding, thus faster, analysis. In the current analysis, estimating the GLM was a relatively quick step, therefore this was no incentive to apply a mask. Another consideration is that since fewer voxels are analysed, there is a smaller chance to find false positives. However, if a mask is applied, brain activity outside of these areas will inherently be missed. Since this was the first fMRI research of tremor in CIDP patients, it was desirable to also detect possible brain activity outside of the cerebello-thalamo-cortical circuit, therefore no mask was applied.

The patterns of brain activity were computed by testing per voxel whether it showed more activity during a task block than in the rest block. Because this involves many comparisons, it is desirable to correct for multiple testing. Consequently, at first the t-test were performed with a FWE-corrected p-value < 0.05. As foreseen, this resulted in no detected clusters of brain activity in three out of four within-group analyses in the first-level analysis. Because the sample size was somewhat limited, the t-tests were also performed with an uncorrected p-value < 0.001, which led to the detection of dozens of clusters. However, it should be kept in mind that in uncorrected testing, you will detect voxels that are false positives. It was decided to apply a cut-off size of 10 voxels in the uncorrected tests and only analyse larger clusters, because it was reasoned that smaller clusters were likely false positive findings. This cut-off value was not applied in the FWE-corrected tests, since more critical testing was performed here reducing the chance of a type I error.

In the group analyses, one participant was analysed in a different group than was determined at inclusion. This participant was moved from the tremor group to the control group, because there was no tremor present during the measurement. Furthermore, the participant whose fMRI data could not be found was also a tremor patient, which explains the unequal number of subjects in the subgroups. As a result, the groups in the analysis were no longer matched 1:1. An alternative approach would have been to remove both the tremor patient and the matched control from the analysis. The matching was not fully as planned throughout all analyses, because sometimes a run was not measured in a participant while it was available from the matched participant. In addition, an error occurred in the processing of one run, which is why this measurement was also removed from the analysis. Regarding the patient who was moved from the tremor to the control group, it could be attempted in future measurements to match two new tremor patient to this patients who was originally included in the tremor group and their matched control participant. Concerning the missing runs, it could be considered to also remove the corresponding measurement from the other subgroup from the analysis to improve the matching of the subgroups, with the disadvantage of reducing the amount of data for the analysis.

4.3 Limitations and further Research

4.3.1 EMG

An original goal of my thesis that was not achieved, was to add a regressor of EMG data to the analysis. Including EMG data in future research is of importance for multiple reasons.
First of all, it allows to separate muscle activity due to tremor from other muscle activity, so that solely the tremor activity can be added as a regressor to the GLM to investigate brain activity related to the tremor. In the current study, this would be especially valuable for the analysis of the dynamic task, because in this task voluntary movement activity was definitely present. Another advantage of adding a regressor of the EMG data to the GLM, is that the severity of tremor activity (measured with the EMG electrodes) would be incorporated into the analysis, via the weight factors of the GLM.

Furthermore, the EMG data could help with qualifying tremor type and hence with deciding what data to include in analyses, and maybe even subgroup allocation. Currently, there was some doubt about the exact tremor activation condition of included patients at time of the measurement. Although all patients had a tremor registration at inclusion to determine this, which showed both postural and intentional tremor in the majority of patients, the tremor during EMG-fMRI acquisition might have been different. As a result, tremor activity in the static or dynamic motor task might have been limited, when in the analysis it was assumed to be present. Additionally, some patients suffered from resting tremor, which means that the assumption of the block design of no activity in the rest blocks was not met. Consequently, tremor activity in the static and dynamic blocks might have been under recognised, since this is computed by comparing the brain activity during a task block with the brain activity during rest blocks. Since the severity, or even presence, of the resting tremor was not clear, it was decided to not exclude those patients. In future research, the EMG data could be used to confirm the tremor type at time of fMRI collection.

In addition to a small variety in activation condition of the tremor among participants, there was also heterogeneity in tremor type. Some patients suffered from tremor, others from myoclonus or a combination of tremor and myoclonus, and in some it was not clear. It would be beneficial to clarify the tremor type of the individual participants prior to a future analysis, possibly with the assistance of the EMG data. If tremor type of each participant is clear, they could be analysed in different subgroups which would help with generalising the results to CIDP patients with either myoclonus or tremor.

Another use of EMG would be to check if the tasks were performed with both hands in all measurements. In the data collected in 2025, all participants performed tasks with both hands, and this is also true for a part of the previously collected data. However, there are reasons to question if this was the case in all measurements, since reports from previous students do mention performing the tasks with the right arm only. In this thesis, clusters of brain activity were mainly detected in the right side of the cerebellum, which makes unilateral execution of the tasks more plausible.

4.3.2 Dynamic Causal Model

The other major direction for future research, besides adding the EMG data to the analysis, is to extend the analysis with a dynamic causal model (DCM). Currently, a GLM was used, in which every voxel is tested to see if it responds to a stimulus, in this case performing a motor task. As a result, brain regions are identified which are functionally connected to the performed task. In a DCM, the influence of different brain areas over one another is studied (79) and also afferent input is included, the so called effective connectivity.(80-82) This is of added value to the research, as information on

how signals propagate through different brain regions could help with the question if the additional brain activity detected in the tremor group is the cause of tremor in these patients, or a reflection of the tremor.

4.4 Clinical Relevance

The results suggests that the cerebello-thalamo-cortical circuit is involved in tremor in CIDP patients, which could give direction to the search for an effective therapy. Currently, tremor in these patients does not respond well to therapy (12), and no guidelines exist yet. Among the participants of this research, one patient used propranolol to suppress tremor, which is the drug of choice for the treatment of essential tremor (83).
In case the central nervous system is involved in CIDP, DBS could be considered for CIDP patients with severe tremor. DBS of the ventral intermediate nucleus of the thalamus (12, 34, 38) and posterior subthalamic area (40) had an effect on tremor in neuropathy patients, although there is a high tolerance risk to the therapy (37). However, the results of this research do not support DBS therapy in CIDP patients, because no activity was found in any of the previously researched targets in DBS.
More research into an effective treatment for tremor in CIDP is necessary, for which based on the results of this thesis, a central mechanism of action should be considered.

5 Conclusion

In this thesis, a potential central pathophysiology of tremor in CIDP patients was investigated. The research was focussed on the cerebello-thalamo-cortical circuit, which plays an important role in motor control and has shown to be involved in the maintenance, and possibly generation, of tremor in other tremor disorders. A fMRI study with a block design was performed, in which brain activity in a static motor task, inducing postural tremor, and a dynamic motor task, inducing intentional tremor, were compared to blocks of rest when no tremor was present.

The between-group results of both tasks suggest that there is more brain activity in the cerebello-thalamo-cortical circuit in CIDP patients who suffer from tremor in comparison to CIDP patients without tremor. The clusters of extra activity were located in cortical and cerebellar areas, but no activity in the thalamus was found in any of the analyses.
A methodological limitation of this research is that the results of the dynamic task may be influenced by a difference in brain activity due to the voluntary tremorlike movement, and therefore cannot be attributed with certainty to tremor activity. Moreover, the heterogeneity of the tremor group limits the generalizability of the results, which could possibly be improved in future analyses.

Further research is necessary to first of all add the simultaneously recorded EMG data as a regressor to the analysis. This allows to separate the brain activity related to tremor from activity resulting from voluntary movement, and enables including the severity of tremor in the fMRI-analysis.
Furthermore, the current GLM analysis could be extended with a DCM, to give insight into if this hyperactivity in the cerebello-thalamo-cortical circuit in CIDP patients with tremor is the cause of tremor, maintaining it, or is a reflection of the tremor of the upper limbs.

References

1. Chang L. Preprocessing 2021 [Available from: https://dartbrains.org/content/Preprocessing.html.
2. Warbrick T SR. A guide to peripheral physiology measurements using the BrainAmp ExG MR - Part 1: Let's focus on EMG 2021 [cited 2025 June 01]. Available from: https://pressrelease.brainproducts.com/emg-fmri/.
3. Jahn A. Chapter 4: Segmentation Andy's Brain Book [cited 2025 June 01]. Available from: https://andysbrainbook.readthedocs.io/en/latest/SPM/SPM_Short_Course/SPM_04_Preprocessing/04_SPM_Segmentation.html.
4. Shastri A, Al Aiyan A, Kishore U, Farrugia ME. Immune-Mediated Neuropathies: Pathophysiology and Management. Int J Mol Sci. 2023;24(8).
5. Zhong Y, Liu H, Liu G, Zhao L, Dai C, Liang Y, et al. A review on pathology, mechanism, and therapy for cerebellum and tremor in Parkinson's disease. NPJ Parkinsons Dis. 2022;8(1):82.
6. Koike H, Katsuno M. Pathophysiology of Chronic Inflammatory Demyelinating Polyneuropathy: Insights into Classification and Therapeutic Strategy. Neurol Ther. 2020;9(2):213-27.
7. Broers MC, Bunschoten C, Nieboer D, Lingsma HF, Jacobs BC. Incidence and Prevalence of Chronic Inflammatory Demyelinating Polyradiculoneuropathy: A Systematic Review and Meta-Analysis. Neuroepidemiology. 2019;52(3-4):161-72.
8. Rodríguez Y, Vatti N, Ramírez-Santana C, Chang C, Mancera-Páez O, Gershwin ME, et al. Chronic inflammatory demyelinating polyneuropathy as an autoimmune disease. J Autoimmun. 2019;102:8-37.
9. Van den Bergh PYK, van Doorn PA, Hadden RDM, Avau B, Vankrunkelsven P, Allen JA, et al. European Academy of Neurology/Peripheral Nerve Society guideline on diagnosis and treatment of chronic inflammatory demyelinating polyradiculoneuropathy: Report of a joint Task Force-Second revision. J Peripher Nerv Syst. 2021;26(3):242-68.
10. Gogia B RCF, Khan Suheb MZ, et al. Chronic Inflammatory Demyelinating Polyradiculoneuropathy. Treasure Island (FL): StatPearls Publishing; 2025 [updated 2024 Mar 4; cited 2025 May 26]. Available from: https://www.ncbi.nlm.nih.gov/books/NBK563249/.
11. Van den Bergh PY, Hadden RD, Bouche P, Cornblath DR, Hahn A, Illa I, et al. European Federation of Neurological Societies/Peripheral Nerve Society guideline on management of chronic inflammatory demyelinating polyradiculoneuropathy: report of a joint task force of the European Federation of Neurological Societies and the Peripheral Nerve Society - first revision. Eur J Neurol. 2010;17(3):356-63.
12. Cao Y, Menon P, Ching-Fen Chang F, Mahant N, Geevasinga N, Fung VS, et al. Postural tremor and chronic inflammatory demyelinating polyneuropathy. Muscle Nerve. 2017;55(3):338-43.
13. Saifee TA, Schwingenschuh P, Reilly MM, Lunn MP, Katschnig P, Kassavetis P, et al. Tremor in inflammatory neuropathies. J Neurol Neurosurg Psychiatry. 2013;84(11):1282-7.
14. Çetinkaya Tezer D, Tutuncu M, Akalin MA, Uzun N, Karaali Savrun F, M EK, et al. Myoclonus and tremor in chronic inflammatory demyelinating polyneuropathy: a multichannel electromyography analysis. Acta Neurol Belg. 2022;122(5):1289-96.
15. Silsby M, Yiannikas C, Fois AF, Kiernan MC, Fung VSC, Vucic S. Upper and lower limb tremor in inflammatory neuropathies. Clin Neurophysiol. 2024;158:69-78.
16. Oaklander AL, Lunn MP, Hughes RA, van Schaik IN, Frost C, Chalk CH. Treatments for chronic inflammatory demyelinating polyradiculoneuropathy (CIDP): an overview of systematic reviews. Cochrane Database Syst Rev. 2017;1(1):Cd010369.
17. Dalakas MC, Teräväinen H, Engel WK. Tremor as a feature of chronic relapsing and dysgammaglobulinemic polyneuropathies. Incidence and management. Arch Neurol. 1984;41(7):711-4.
18. Busby M, Nithi K, Mills K, Donaghy M. The tremor associated with non-paraproteinaemic acquired demyelinating polyneuropathy--a case study. J Neurol. 2003;250(4):486-7.

19. Dalakas MC, Engel WK. Chronic relapsing (dysimmune) polyneuropathy: pathogenesis and treatment. Ann Neurol. 1981;9 Suppl:134-45.
20. Silsby M, Fois AF, Yiannikas C, Ng K, Kiernan MC, Fung VSC, et al. Chronic inflammatory demyelinating polyradiculoneuropathy-associated tremor: Phenotype and pathogenesis. Eur J Neurol. 2023;30(4):1059-68.
21. Brooks D, Jenkins I, Bain P, Colebatch J, Thompson P, Findley L, et al. A comparison of the abnormal patterns of cerebral activation associated with neuropathic and essential tremor. Neurology. 1992;42(Suppl 3):423.
22. Bain PG, Britton TC, Jenkins IH, Thompson PD, Rothwell JC, Thomas PK, et al. Tremor associated with benign IgM paraproteinaemic neuropathy. Brain. 1996;119 (Pt 3):789-99.
23. Stanton M, Pannoni V, Lewis RA, Logigian EL, Naguib D, Shy ME, et al. Dispersion of compound muscle action potential in hereditary neuropathies and chronic inflammatory demyelinating polyneuropathy. Muscle Nerve. 2006;34(4):417-22.
24. Kiers L, Clouston P, Zuniga G, Cros D. Quantitative studies of F responses in Guillain-Barré syndrome and chronic inflammatory demyelinating polyneuropathy. Electroencephalogr Clin Neurophysiol. 1994;93(4):255-64.
25. Wasielewska A, Rudzińska M, Tomaszewski T, Banaszkiewicz K, Wójcik-Pędziwiatr M, Dec-Ćwiek M, et al. Tremor in neuropathies of different origin. Neurol Neurochir Pol. 2013;47(6):525-33.
26. Pedersen SF, Pullman SL, Latov N, Brannagan TH, 3rd. Physiological tremor analysis of patients with anti-myelin-associated glycoprotein associated neuropathy and tremor. Muscle Nerve. 1997;20(1):38-44.
27. Schwingenschuh P, Katschnig P, Edwards MJ, Teo JT, Korlipara LV, Rothwell JC, et al. The blink reflex recovery cycle differs between essential and presumed psychogenic blepharospasm. Neurology. 2011;76(7):610-4.
28. Schwingenschuh P, Saifee TA, Katschnig-Winter P, Reilly MM, Lunn MP, Manji H, et al. Cerebellar learning distinguishes inflammatory neuropathy with and without tremor. Neurology. 2013;80(20):1867-73.
29. Bracha V, Zhao L, Wunderlich DA, Morrissy SJ, Bloedel JR. Patients with cerebellar lesions cannot acquire but are able to retain conditioned eyeblink reflexes. Brain. 1997;120 (Pt 8):1401-13.
30. Hoffland BS, Bologna M, Kassavetis P, Teo JT, Rothwell JC, Yeo CH, et al. Cerebellar theta burst stimulation impairs eyeblink classical conditioning. J Physiol. 2012;590(4):887-97.
31. Christian KM, Thompson RF. Neural substrates of eyeblink conditioning: acquisition and retention. Learn Mem. 2003;10(6):427-55.
32. Querol L, Nogales-Gadea G, Rojas-Garcia R, Diaz-Manera J, Pardo J, Ortega-Moreno A, et al. Neurofascin IgG4 antibodies in CIDP associate with disabling tremor and poor response to IVIg. Neurology. 2014;82(10):879-86.
33. Bayreuther C, Delmont E, Borg M, Fontaine D. Deep brain stimulation of the ventral intermediate thalamic nucleus for severe tremor in anti-MAG neuropathy. Mov Disord. 2009;24(14):2157-8.
34. Breit S, Wächter T, Schöls L, Gasser T, Nägele T, Freudenstein D, et al. Effective thalamic deep brain stimulation for neuropathic tremor in a patient with severe demyelinating neuropathy. J Neurol Neurosurg Psychiatry. 2009;80(2):235-6.
35. McMaster J, Gibson G, Castro-Prado F, Vitali A, Honey CR. Neurosurgical treatment of tremor in anti-myelin-associated glycoprotein neuropathy. Neurology. 2009;73(20):1707-8.
36. Růzicka E, Jech R, Zárubová K, Roth J, Urgosík D. VIM thalamic stimulation for tremor in a patient with IgM paraproteinaemic demyelinating neuropathy. Mov Disord. 2003;18(10):1192-5.
37. Patel N, Ondo W, Jimenez-Shahed J. Habituation and rebound to thalamic deep brain stimulation in long-term management of tremor associated with demyelinating neuropathy. Int J Neurosci. 2014;124(12):919-25.
38. Cabañes-Martínez L, Del Álamo de Pedro M, de Blas Beorlegui G, Bailly-Bailliere IR. Long-Term Effective Thalamic Deep Brain Stimulation for Neuropathic Tremor in Two Patients with Charcot-Marie-Tooth Disease. Stereotact Funct Neurosurg. 2017;95(2):102-6.

39. Vial F, Kassavetis P, Merchant S, Haubenberger D, Hallett M. How to do an electrophysiological study of tremor. Clin Neurophysiol Pract. 2019;4:134-42.
40. Blomstedt P, Fytagoridis A, Tisch S. Deep brain stimulation of the posterior subthalamic area in the treatment of tremor. Acta Neurochir (Wien). 2009;151(1):31-6.
41. Dirkx MF, den Ouden H, Aarts E, Timmer M, Bloem BR, Toni I, et al. The Cerebral Network of Parkinson's Tremor: An Effective Connectivity fMRI Study. J Neurosci. 2016;36(19):5362-72.
42. Dirkx MF, Zach H, van Nuland A, Bloem BR, Toni I, Helmich RC. Cerebral differences between dopamine-resistant and dopamine-responsive Parkinson's tremor. Brain. 2019;142(10):3144-57.
43. Horne MK, Butler EG. The role of the cerebello-thalamo-cortical pathway in skilled movement. Prog Neurobiol. 1995;46(2-3):199-213.
44. Helmich RC, Hallett M, Deuschl G, Toni I, Bloem BR. Cerebral causes and consequences of parkinsonian resting tremor: a tale of two circuits? Brain. 2012;135(Pt 11):3206-26.
45. Helmich RC, Toni I, Deuschl G, Bloem BR. The pathophysiology of essential tremor and Parkinson's tremor. Curr Neurol Neurosci Rep. 2013;13(9):378.
46. Awad A, Blomstedt P, Westling G, Eriksson J. Deep brain stimulation in the caudal zona incerta modulates the sensorimotor cerebello-cerebral circuit in essential tremor. Neuroimage. 2020;209:116511.
47. Juttukonda MR, Franco G, Englot DJ, Lin YC, Petersen KJ, Trujillo P, et al. White matter differences between essential tremor and Parkinson disease. Neurology. 2019;92(1):e30-e9.
48. Madelein van der Stouwe AM, Nieuwhof F, Helmich RC. Tremor pathophysiology: lessons from neuroimaging. Curr Opin Neurol. 2020;33(4):474-81.
49. Nieuwhof F, Panyakaew P, van de Warrenburg BP, Gallea C, Helmich RC. The patchy tremor landscape: recent advances in pathophysiology. Curr Opin Neurol. 2018;31(4):455-61.
50. Tsuboi T, Jabarkheel Z, Foote KD, Okun MS, Wagle Shukla A. Importance of the initial response to GPi deep brain stimulation in dystonia: A nine year quality of life study. Parkinsonism Relat Disord. 2019;64:249-55.
51. Merola A, Dwivedi AK, Shaikh AG, Tareen TK, Da Prat GA, Kauffman MA, et al. Head tremor at disease onset: an ataxic phenotype of cervical dystonia. J Neurol. 2019;266(8):1844-51.
52. Sedov A, Usova S, Semenova U, Gamaleya A, Tomskiy A, Beylergil SB, et al. Pallidal Activity in Cervical Dystonia with and Without Head Tremor. Cerebellum. 2020;19(3):409-18.
53. Richardson MP, Grosse P, Allen PJ, Turner R, Brown P. BOLD correlates of EMG spectral density in cortical myoclonus: description of method and case report. Neuroimage. 2006;32(2):558-65.
54. van Rootselaar AF, Maurits NM, Renken R, Koelman JH, Hoogduin JM, Leenders KL, et al. Simultaneous EMG-functional MRI recordings can directly relate hyperkinetic movements to brain activity. Hum Brain Mapp. 2008;29(12):1430-41.
55. Contarino MF, Groot PF, van der Meer JN, Bour LJ, Speelman JD, Nederveen AJ, et al. Is there a role for combined EMG-fMRI in exploring the pathophysiology of essential tremor and improving functional neurosurgery? PLoS One. 2012;7(10):e46234.
56. Bucher SF, Seelos KC, Dodel RC, Reiser M, Oertel WH. Activation mapping in essential tremor with functional magnetic resonance imaging. Ann Neurol. 1997;41(1):32-40.
57. Sharifi S, Luft F, de Boer L, Buijink AWG, Mugge W, Schouten AC, et al. Closing the loop: Novel quantitative fMRI approach for manipulation of the sensorimotor loop in tremor. Neuroimage. 2022;262:119554.
58. Helmich RC, Bloem BR, Toni I. Motor imagery evokes increased somatosensory activity in Parkinson's disease patients with tremor. Hum Brain Mapp. 2012;33(8):1763-79.
59. European Federation of Neurological Societies/Peripheral Nerve Society Guideline on management of paraproteinemic demyelinating neuropathies. Report of a Joint Task Force of the European Federation of Neurological Societies and the Peripheral Nerve Society--first revision. J Peripher Nerv Syst. 2010;15(3):185-95.
60. Brainard DH. The Psychophysics Toolbox. Spat Vis. 1997;10(4):433-6.
61. van der Meer JN, Tijssen MA, Bour LJ, van Rootselaar AF, Nederveen AJ. Robust EMG-fMRI artifact reduction for motion (FARM). Clin Neurophysiol. 2010;121(5):766-76.

62. Stoodley CJ, Valera EM, Schmahmann JD. Functional topography of the cerebellum for motor and cognitive tasks: an fMRI study. Neuroimage. 2012;59(2):1560-70.
63. Grodd W, Hülsmann E, Lotze M, Wildgruber D, Erb M. Sensorimotor mapping of the human cerebellum: fMRI evidence of somatotopic organization. Hum Brain Mapp. 2001;13(2):55-73.
64. Weiner KS, Zilles K. The anatomical and functional specialization of the fusiform gyrus. Neuropsychologia. 2016;83:48-62.
65. Park IS, Lee NJ, Rhyu IJ. Roles of the Declive, Folium, and Tuber Cerebellar Vermian Lobules in Sportspeople. J Clin Neurol. 2018;14(1):1-7.
66. Parent A, Hazrati LN. Functional anatomy of the basal ganglia. I. The cortico-basal ganglia-thalamo-cortical loop. Brain Res Brain Res Rev. 1995;20(1):91-127.
67. Alexander GE, DeLong MR, Strick PL. Parallel organization of functionally segregated circuits linking basal ganglia and cortex. Annu Rev Neurosci. 1986;9:357-81.
68. Uddin LQ, Nomi JS, Hébert-Seropian B, Ghaziri J, Boucher O. Structure and Function of the Human Insula. J Clin Neurophysiol. 2017;34(4):300-6.
69. Hartwigsen G, Neef NE, Camilleri JA, Margulies DS, Eickhoff SB. Functional Segregation of the Right Inferior Frontal Gyrus: Evidence From Coactivation-Based Parcellation. Cereb Cortex. 2019;29(4):1532-46.
70. Herrero MT, Barcia C, Navarro JM. Functional anatomy of thalamus and basal ganglia. Childs Nerv Syst. 2002;18(8):386-404.
71. Buijink AW, van der Stouwe AM, Broersma M, Sharifi S, Groot PF, Speelman JD, et al. Motor network disruption in essential tremor: a functional and effective connectivity study. Brain. 2015;138(Pt 10):2934-47.
72. Broersma M, van der Stouwe AMM, Buijink AWG, de Jong BM, Groot PFC, Speelman JD, et al. Bilateral cerebellar activation in unilaterally challenged essential tremor. Neuroimage Clin. 2016;11:1-9.
73. Parker DB, Razlighi QR. The Benefit of Slice Timing Correction in Common fMRI Preprocessing Pipelines. Front Neurosci. 2019;13:821.
74. neuroimaging Wch. fMRI data preprocessing: Slice timing correction [cited 2025 May 28]. Available from: https://www.fil.ion.ucl.ac.uk/spm/docs/tutorials/fmri/block/preprocessing/slice_timing/.
75. neuroimaging Wcfh. fMRI data preprocessing [cited 2025 May 28]. Available from: https://www.fil.ion.ucl.ac.uk/spm/docs/tutorials/fmri/block/preprocessing/introduction/.
76. Jahn A. fMRI Introduction 2025 [cited 2025 May 28]. Available from: https://andysbrainbook.readthedocs.io/en/latest/fMRI_Short_Course/fMRI_Intro.html.
77. Carp J. The secret lives of experiments: methods reporting in the fMRI literature. Neuroimage. 2012;63(1):289-300.
78. Churchill NW, Spring R, Afshin-Pour B, Dong F, Strother SC. An Automated, Adaptive Framework for Optimizing Preprocessing Pipelines in Task-Based Functional MRI. PLoS One. 2015;10(7):e0131520.
79. Friston K. Causal modelling and brain connectivity in functional magnetic resonance imaging. PLoS Biol. 2009;7(2):e33.
80. Kahan J, Foltynie T. Understanding DCM: Ten simple rules for the clinician. NeuroImage. 2013;83.
81. Friston KJ. Functional and effective connectivity: a review. Brain Connect. 2011;1(1):13-36.
82. Supat S, Rosas F, Yousuke O, Yoshimura N, Koike Y. Comparison of resting-state functional and effective connectivity between default mode network and memory encoding related areas. Journal of Neuroscience and Neurological Disorders. 2020;4:029-37.
83. Pal PK. Guidelines for management of essential tremor. Ann Indian Acad Neurol. 2011;14(Suppl 1):S25-8.

Appendices

Appendix A: FARM Algorithm

A.1 Reasons to use FARM for EMG-fMRI data

In addition to being able to process multi slice data, there are two other reasons why the Robust EMG-fMRI artifact reduction for motion (FARM) is suitable for removing the MR artifact from the EMG data. One of them being that the algorithm has been developed for EMG data. Commonly, EEG-fMRI techniques are used which focus on artifact removement below 50Hz, since most important EEG frequencies are below this threshold (1, 2). These techniques are translatable to EMG-fMRI data to some extent, as similar artifacts are present in EEG and EMG data collected in MR environment. However, EMG content ranges up to approximately 250Hz (26) so artifact removement in higher frequencies is desired too. For artifact removement at these higher frequencies, synchronization between the EMG amplifier and the MRI scanner is critical and the FARM algorithm focusses on this (4).

Furthermore, FARM can remove the MR artifact while movement is performed. In a static situation, the MR artifact is generated by interaction between the gradient of the MRI scanner and electrodes used for recording EMG. The total artifact can be divided in an artifact which repeats every fMRI volume, and one that is related to every acquired slice. When movements are performed while scanning, the shape of the artifact changes due to movement of the electrodes within the magnetic field. In a static task, the artifact has a periodicity which enables artifact removement based on a template of the artifact. As a result of movement the shape of the artifact changes unpredictably, requiring a more complex approach.(4)

A.2 Steps of the FARM algorithm

In the FARM workflow, pre- and post processing are performed prior to and after the actual FARM algorithm. All steps are performed in Matlab, and the EEGLAB toolset was used to load in the data. The pre-processing consists of multiple parts, of which the first is to constructs bipolar EMG from monopolar channels. The data in this project was acquired with bipolar electrodes, so this step was unnecessary. Next, the data is high-pass filtered above 30Hz, to remove the artifact due to motion. While recording the EMG-fMRI data, triggers for the start of each volume were stored into the EMG data. Additionally, there are artifacts related to each slice too. To remove these, the algorithm inserts slice-onset markers into the EMG data. Simultaneously, it generates estimates for the duration of each slice. The final pre-processing step is to up-sample the data.

Following pre-processing, FARM was applied to the remaining signal. In the FARM method, three operations are performed to remove the MR artifact. Firstly, the slice markers inserted in pre-processing are optimized to improve slice-alignment. Secondly, volume-artifact correction is performed. Since volume and slice artifacts partly overlap, removing volume-artifact influences the concurrent slice-artifact. To correct for this, the affected slice-artifact was substituted with periods of raw data. Thirdly, slice-templated were formed and subtracted from the signal using a relatively large sliding window of 50 slice-segments from which slice-artifacts with highest correlation were selected.

The FARM method was ended with post-processing of the signal which entailed down-sampling and a 250Hz low-pass filter.

A.3 EMG Pre-processing

Getting acquainted with the data and the FARM code, and making the code run was challenging. During the EMG-fMRI measurement, EMG was recorded from four muscles and additionally ground electrodes were applied. Furthermore, a trigger channel with information when the fMRI scans were obtained, was expected. However, the EMG data set of many participants consisted of more channels than expected. Possibly, the accelerometry data, which was recorded along with EMG-fMRI in 2019-2021, was included in the EMG data set too. This will need to be explored in more depth in the future. Another observation in the EMG data was that there were more triggers per run present than acquired scan volumes. First, there were 696 consecutive triggers, followed by approximately 40 more triggers after a short break. No explanation of the additional triggers has been found, but it is thought that these can be ignored and that the EMG of the first 696 triggers corresponds to the fMRI data. After the data was loaded into EEGLAB, a start with the FARM algorithm was made. Slice triggers were added to the data, but subsequent steps were not accomplished due to time restriction.

A.4 References

1. Ritter P, Becker R, Graefe C, Villringer A. Evaluating gradient artifact correction of EEG data acquired simultaneously with fMRI: 2007. Elsevier Science Inc.; 2007. p. 923–32.
2. Dressler O, Schneider G, Stockmanns G, Kochs EF. Awareness and the EEG power spectrum: analysis of frequencies. Br J Anaesth 2004;93(6)

:806–9.
3. Myers LJ, Lowery M, O'Malley M, Vaughan CL, Heneghan C, Gibson ASC, et al. Rectification and non-linear pre-processing of EMG signals for cortico-muscular analysis. J Neurosci Methods 2003;124(2):157–65.
4. van der Meer JN, Tijssen MA, Bour LJ, van Rootselaar AF, Nederveen AJ. Robust EMG-fMRI artifact reduction for motion (FARM). Clin Neurophysiol. 2010 May;121(5):766-76. doi: 10.1016/j.clinph.2009.12.035. Epub 2010 Feb 8. PMID: 20117046.

Appendix B: Current Methods for a combined EMG-fMRI Analysis in Patients with Tremor of the upper Limb (Literature study TM30001)

Introduction

Functional Magnetic Resonance Imaging (1) can be used to assess brain activity non-invasively. The most widely used technique in fMRI is to measure oxygen consumption of the brain, which indicates activity, based on blood oxygen level-dependent (BOLD) contrast.(2) fMRI studies can provide insight into the relation between movements and brain activity, if a motor task is performed by the subject during fMRI scanning. A common way to set-up such a study is using a block-design, in which blocks of motor task(s) are alternated with rest.(3) In the analysis, the fMRI images acquired during a task block or rest block are evaluated separately, which enables comparison of brain activity between the different conditions.

If additionally surface electromyography (EMG) is recorded simultaneously with fMRI acquisition (EMG-fMRI), this offers extra opportunities for the analysis. First of all, combined EMG-fMRI analysis allows to accurately determine the start and end of a task or rest block. Furthermore, it provides information on the execution of the task and additional muscle contractions of a subject at any moment within the EMG-fMRI acquisition.(3, 4) Overall, with simultaneous EMG-fMRI the relation between movement and brain activity can be studied in detail and more directly than with fMRI only, utilizing the high spatial resolution of fMRI imaging and high temporal resolution of EMG(2).

A combined EMG-fMRI analysis is especially of added value when studying brain activity in tasks with a variance in execution, such as motor tasks in patients with tremor. A challenge is to distinguish between brain activations because of the performed motor task and simultaneous involuntary tremor movement(3). The study design can help to some extent with making this separation, for example by recording rest tremor in Parksinson's Disease (PD) patients when they are in rest, so theoretically no voluntary movement is involved in the measurement. Unfortunately, this experimental set-up leaves some opportunities for improvement, since there is also neuronal activity due to afferent sensory input present in tremor, which is not easily differentiated from brain activity resulting from tremor movement(1, 5). In case of a postural or action tremor, such as in essential tremor (ET) patients, it is even more complex to distinguish between brain activity related to voluntary movement and tremor, because they co-occur. However, earlier research has shown that amplitude variations in EMG data, after certain processing steps of the data have been performed, reflects extra EMG activity induced by the tremor(3, 6). When this EMG variable is used as a regressor in the EMG-fMRI analysis, the relation between tremor-related EMG information and BOLD activity in the brain can be researched more reliably(4).

For my thesis, I will use EMG-fMRI data to investigate the pathophysiology of tremor in chronic inflammatory demyelinating polyneuropathy patients. CIDP is the most common immune-mediated neuropathy worldwide(7) with a prevalence ranged between 0.67 and 10.3 per 100,000 (8), and is clinically heterogeneous(7). A considerable part of CIDP patients suffer from a disabling neuropathic tremor, which has been described as an action tremor with a low frequency and high amplitude, and can be a postural or intentional tremor. In some CIDP patients, rest tremor is present too. (9, 10) The pathophysiology of tremor in neuropathy is unknown, and multiple origins are hypothesized. During my thesis I will contribute to research of a potential central origin of tremor in CIDP patients. The research protocol for the EMG-fMRI measurements has already been written and approved by a medical ethics assessment committee (METC). Therefore, choosing a method for safely recording EMG simultaneously with fMRI, and preprocessing steps to correct EMG data for artifacts caused by the gradient of the fMRI scan, are not a part of my thesis and hence not the focus of this literature

review. However, the method for using the EMG data as a regressor in the fMRI analysis has not been determined yet, while this analysis will be of importance for my thesis. In preparation for my thesis, the aim of this article is to review current methods for a combined EMG-fMRI analysis in patients with tremor of the upper limb.

Methods

Search strategy

Pubmed was searched on October 21st 2024 for studies that focused on EMG-fMRI. A combination of the words 'fMRI' or 'functional MRI', and 'EMG' or 'electromyography' in the title or abstract of the articles were used for the search. Additionally, the reference lists of the included studies were reviewed for relevant studies that the search strategy potentially missed.

Study selection

Titles and abstract of all articles that resulted from the PubMed search were screened for eligibility. In case of uncertainty, the methods section of the article was read too. Publications were included if EMG and fMRI data were acquired simultaneously in human participants, and excluded if there was no full text available in English. Subsequently, the inclusion was narrowed down to studies with participants who suffered from movement disorders of the upper limb, and used EMG as a regressor in the fMRI analysis.

Data extraction

The following study characteristics were extracted from the eligible studies: first author, year of publication, diagnosis of subjects, and number of subjects. For the data acquisition, the executed task, location of EMG electrodes and fMRI settings were collected. About the data analysis, the region of interest in the brain for the fMRI analysis, and the method of using EMG as a regressor for the fMRI analysis was extracted.

Results

Search results

The search in PubMed resulted in 204 publications (Figure 1). After screening of the title, abstract, and occasionally method section, 136 studies were excluded because they did not meet the criteria. In a majority of these excluded studies (n=128), electromyography and fMRI were not acquired simultaneously. The remaining 68 articles were screened again. This second selection round resulted in the exclusion of 57 articles. 51 were excluded based on the characteristics of the participants (healthy participants (n=25), not movement disorder patients (n=23), blepharospasm (n=3)). A couple studies did not meet the criteria because they focused on either the recording or artifact correction of EMG acquired during fMRI, instead of the EMG-fMRI analysis (n=4), or EMG was analyzed separately from the fMRI scan analysis (n=1), or EMG was used as a nuisance variable in the fMRI analysis (n=1). The reference list of included studies did not lead to any new inclusions, resulting in a total of 11 included studies.

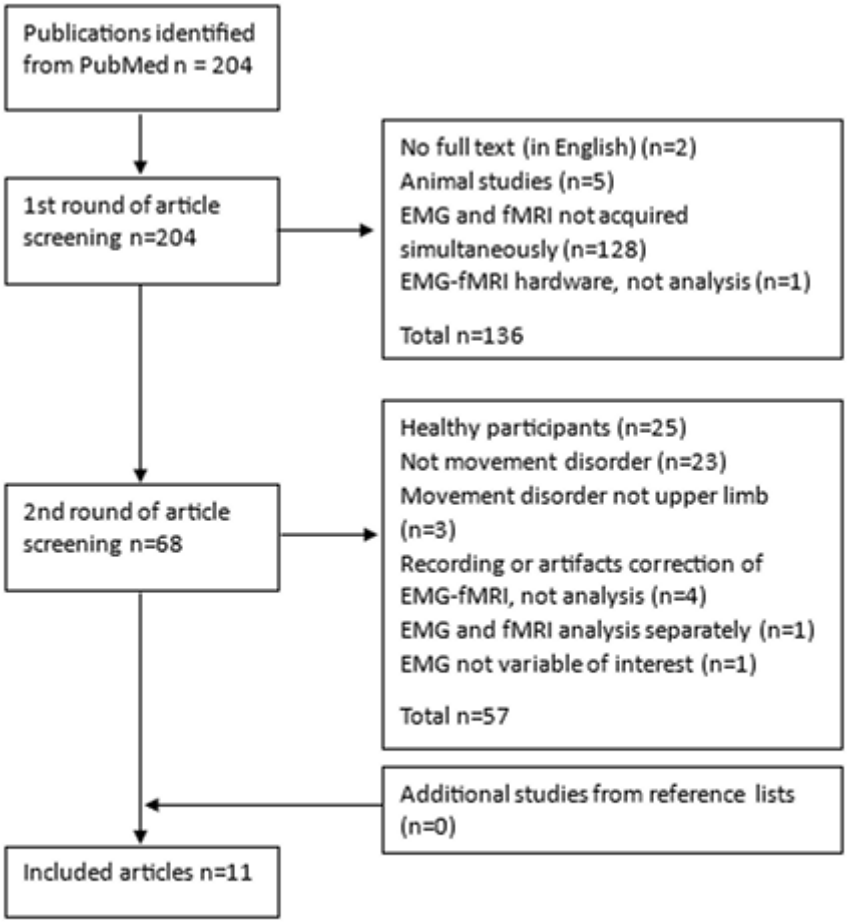

Figure 1: Flowchart of study inclusion

Study characteristics

Included articles were published between 2006 and 2022. The number of participants varied between n=1 and n=55, and the most common movement disorder diagnosis among the articles was tremor-dominant Parkinson's Disease (PD)(5, 6, 11-14), followed by essential tremor (ET)(4, 5, 15, 16). Five articles included healthy (matched) controls in their research(3, 5, 6, 15, 16), one article additionally compared tremulous- and nontremor PD patients(6), and one study compared dopamine-responsive and dopamine-resistant tremor in PD(13).

Experiment set-up

Eight of the studies were set-up (Table 2) with a block design, alternating rest and tasks or different tasks. In three articles, all participants performed extension of the arms and fingers, often with pronated hands(2-4). In two of these articles, this task was alternated with self-paced flexion-extension movements of the wrist (3, 4). Richardson et al. (2) did not have a second task, they compared the extension with rest. In two other articles, both with a group of ET patients and healthy controls, only the ET patients performed the extension of arms and fingers task, evoking tremor. Meanwhile the control participants were asked to mimic a tremor with self-paced flexion-extension movements. (15, 16) One study involved a wrist manipulator, in which participants either followed its movement, or tried to work against it, alternated with rest(5).

In five articles, no movement task was involved (6, 11-14). Instead, the participants were measured in

rest. In two studies the rest was alternated with mental load (13, 14), and in one study participants performed imaginary motor tasks(6).

Table 1: Study characteristics

Author, year	**Participants**	
	Movement disorder diagnosis	*Number of subjects*
Richardson, 2006	Familial cortical tremor	n=1
Van Rootselaar, 2008	FCMTE	FCMTE: n=8 Control: n=9
Contarino, 2012	ET with unilateral thalamotomy	n=6
Helmich, 2012	Tremor-dominant and non-tremor PD	Tremor-dominant PD: n=18 Non-tremor PD: n=20 Control: n=19
Broersma, 2015	ET	ET: n=21 Control: n=21
Buijink, 2015	ET	ET: n=21 Control: n=22
Dirkx, 2016	Tremor-dominant PD	C1: n=19 C2: n=22
Dirkx, 2017	Tremor-dominant PD	n=15
Dirkx, 2019	PD, dopamine-responsive tremor and dopamine resistant tremor	Dopamine-responsive tremor: n=20 Dopamine-resistant tremor: n=14
Dirkx, 2020	Tremor-dominant PD	n=33
Sharifi, 2022	ET, tremor-dominant PD	ET: n=18 PD: n=14 Control: n=18

FCMTE = familial cortical myoclonic tremor with epilepsy; ET = essential tremor; PD = Parkinson's Disease; C = cohort

EMG electrode location

In a majority of the studies, EMG was recorded from at least two forearm muscles to gain information about wrist flexion and extension. (See Table 2) The most commonly recorded flexor among the studies was the m. flexor carpi radialis(4, 5, 11-16). Across the articles, the recorded extensor varied. In two studies, the recorded muscles depended on the patient specific tremor. Contarino et al measured the EMG from two forearm muscles with the strongest tremor, in addition to the EMG recordings of the m. extensor- and m. flexor carpi radialis(4). Helmich et al. (6) recorded EMG from one muscle of the most affected arm, either the extensor digitorum communis or the flexor carpi radialis, depending on the tremor characteristics.

In the articles by Dirkx et al. (11-14) and Helmich et al. (6), no motor task was performed and EMG was recorded from the most affected arm. Contarino et al.(4) and Richardson et al.(2) asked their participants to perform motor tasks with both the left and right arms and recorded EMG from both arms. Broersma et al.(16) also recorded EMG from both arms. However, the recordings from the left arm were to verify relaxation of this side while tasks were performed with the right arm. In the other studies, motor tasks and EMG recordings were performed on the right side only. In some studies, right-handed participants were selected for the experiment(5, 15, 16).

Table 2: Study set-up and data-acquisition

Author, year	**Study set-up**	**Data-acquisition**	
		Location EMG electrodes	*fMRI settings*
Richardson, 2006	Rest; Sustained: extended hands with fingers spread	Left and right: -Brachioradialis -First dorsal interosseous	TE: 40ms TR: 2.5s VD: 3x3x3.67mm
Van Rootselaar, 2008	Rest; Posture: extension and pronation of right arm, hand, and fingers; Movement: self-paced wrist flexion–extension, divided in ''fast'' movement and ''slow'' movement, keeping arm extended	Right: -Wrist extensor muscles; -First dorsal interosseus muscle and metacarpophalangeal joint	EPI: single shot TE: 35ms TR: 3s slice thickness: 3.5mm
Contarino, 2012	Movement: self-paced wrist flexion-extension, stretched arm; Tremor: stretched arm with pronated hand and extended wrist and fingers.	Both arms: -Extensor carpi radialis; -Flexor carpi radialis; -Two other arm muscles with strongest tremor	Not reported
Helmich, 2012	Motor imagery task	Most affected arm, based on tremor characteristics: -Extensor digitorum communis or -Flexor carpi radialis	EPI: single shot TE: 30ms TR: 2.38s VD: 3.5x3.5x3mm
Broersma, 2015	Rest; Task: -ET: right hand and arm extension; -Control: mimic tremor by self-paced wrist flexion-extension.	Right arm muscles: -Extensor carpi ulnaris; -Flexor carpi radialis; -Extensor carpi radialis longus; -Flexor carpi ulnaris; -First dorsal interosseus	EPI: multi slice TE: 30ms TR: 2s VD: 3.5x3.5x3.5mm
Buijink, 2015	Rest; Rask: -ET: right hand and arm extension; -Control: mimic tremor by self-paced flexion-extension; Additional reading task during half of task blocks	Right (dominant) hand: 5 right arm muscles	EPI: multi-slice TE: 30ms TR: 2s
Dirkx, 2016	Rest	Most affected forearm: -Extensor digitorum communis; -Flexor carpi radialis muscles	EPI: single shot/multi-slice TE: 30/ TE1: 9.4 /TE2: 21.2 /TE3: 33 /TE4: 45 ms TR: 1450/1820ms VD: 3.5x3.5x5 / 3.5x3.5x3mm

Dirkx, 2017	Rest	Most affected forearm: -Extensor digitorum communis; -Flexor carpi radialis muscles	EPI: multi-slice TE: TE1: 9.4 /TE2: 21.2s/TE3: 33/TE4: 45 ms TR: 1820ms VD: 3.5x3.5x3mm
Dirkx, 2019	Rest; Cognitive stress (arithmetic)	Most affected forearm: -Extensor digitorum communis; -Flexor carpi radialis muscles	EPI: multi-band TE: 34ms TR: 0.859s VD: 2.2x2.2x2.2mm
Dirkx, 2020	Rest; Cognitive stress (arithmetic)	Most affected forearm: -Extensor digitorum communis; -Flexor carpi radialis muscles	EPI: multi-band TE: 34ms TR: 0.859s VD: 2.2x2.2x2.2mm
Sharifi, 2022	Wrist manipulator: (1) active motor task: intentionally counteract the wrist manipulator; (2) passive movement task: undergo the wrist manipulator; (3) rest, without any wrist movement or activity.	Right (dominant) hand: -Extensor carpi ulnaris; -Flexor carpi radialis; -First dorsal interosseous muscles	TE: 30ms TR: 2s VD: 3.5x3.5x3.5mm

*EPI = echo planar imaging; VD = voxel dimensions; *C1/C2*

Table 3: Data analysis

Author, year	***ROI/network***	***EMG regressor***								
		Channel(s)	*Frequency*	*Spectral power*	*Orthogona-lization*	*Log. values*	*Normali-zation*	*Scaling*	*HRF*	*Model*
Richardson, 2006	Whole brain	All	6-30Hz 31-100Hz	Yes		Yes			Yes	GLM
Van Rootselaar, 2008	Whole brain	Best artifact correction	1-250Hz	Yes	Yes			Yes	Yes	GLM
Contarino, 2012	Thalamus mask: thalamus only; Circuit mask: thalamus, putamen, caudate, cerebellum, brainstem	Best artifact correction Clear tremor activity	1-250Hz* Tremor freq.**	Yes	Yes				Yes	GLM
Helmich, 2012	Whole brain; ROI: bilateral dorsal premotor cortex	All	Tremor freq.	Yes			Yes		Yes	GLM
Broersma, 2015	Whole brain; Cerebellum mask	Average of 3 channels with highest power	Tremor freq. ± 2.5Hz	Yes	Yes			Yes	Yes	GLM
Buijink, 2015	Whole brain mask; Whole cerebellum mask; Cerebral motor mask	Average of 3 channels with highest power	Tremor freq. ± 2.5Hz	Yes	Yes			Yes	Yes	GLM, DCM
Dirkx, 2016	Contralateral GPe, GP), STN, primary MC, VIM; Ipsilateral cerebellum	Not reported	Tremor freq.	Yes		Yes	Yes		Yes	GLM, DCM
Dirkx, 2017	Cerebello-thalamo-cortical motor circuit: MC (Brodmann area), VIM, cerebellum; Basal ganglia: GPi, GPe; STN	Not reported	Tremor freq.	Yes		Yes	Yes		Yes	GLM, DCM
Dirkx, 2019	Contralateral: MC (Brodmann area), VLpv, GPe, GPi Ipsilateral cerebellum	Not reported	Tremor freq. ± 1.5Hz	Yes		Yes	Yes		Yes	GLM, DCM
Dirkx, 2020	Contralateral: MC (Brodmann area), VLpv,, GPe, GPi Ipsilateral cerebellum	Not reported	Tremor freq.	Yes		Yes	Yes		Yes	GLM, DCM
Sharifi, 2022	Sensorimotor mask, incl.: -primary MC, primary somatosensory cortex, sensorimotor association areas (premotor cortex, Brodmann), secondary sensory areas (operculum), cerebellum (anterior lobe and lobule VIII), basal ganglia, thalamus	Highest peak around tremor freq.	Tremor freq. ± 2.5Hz	Yes	Yes		Yes		Yes	GLM

*ROI: region of interest; HRF: hemodynamic response function; freq.: frequency; *movement protocol; **tremor protocol; GPe: external globus pallidus; GPi: internal globus pallidus; STN: subthalamic nucleus; MC: motor cortex; VIM: thalamic intermediate nucleus; VLpv: centrolateral thalamus*

fMRI settings

T2*-weighted echo planar imaging fMRI scans were obtained in all articles, using single shot (3, 6, 11), multi-slice(11, 12, 15, 16) or multi-band(13, 14) echo planar imaging (EPI) (Table 2). The echo time (TE) varied between 30 and 40ms, and the repetition time (TR) between 0.859 and 3s. The most commonly reported voxel size differed between 3-3.67mm^3 (2, 6, 11, 12, 16). However, in two of the studies by Dirkx et al.(13, 14) an isotropic voxel of 2.2mm^3 was used. In addition to the functional images, T1-weighted anatomical MRI scan were made in all studies to provide anatomical information with a high spatial resolution (voxel size of 1mm^3 (3, 5, 6, 11, 13, 14, 16)).

ROI/network brain

Some of the studies performed a whole brain search to investigate changes in brain activity during different test conditions (2, 3, 6, 13, 15, 16), others focused on a specific region or network of interest (ROI) in their analysis(4-6, 11-16) (Table 3).

Two articles focused on developing(2) and verifying(3) techniques which allow combined EMG-fMRI analysis in tremor patients, for which they performed a whole brain analysis.

In addition to a whole brain search, Helmich et al.(6) performed a ROI analysis on the bilateral dorsal premotor cortex (PMd), since they expected to find differences between tremor and nontremor PD in the PMd. Broersma et al.(16) also combined a whole brain analysis with a ROI analysis. However, their ROI was the cerebellum, as they aimed to localize cerebellar abnormalities in ET patients.

Various articles studied the cerebello-thalamo-cortical network, which is recognized to be involved in tremor(4, 5, 11-15). Which (part of) brain structures of this loop were studied differed slightly among the articles, more details can be found in Table 2.

EMG as regressor variable

After fMRI- and movement artifact correction was performed on the EMG recordings, which is outside the scope of this review, the EMG recordings were further processed to be used as regressors in the fMRI analysis.

The first two steps were selecting EMG channel(s) and a frequency band of interest for the analysis. Some articles used all recorded EMG channels for the analysis(2, 6), others made a selection. Van Rootselaar et al. (3) and Contarino et al. (4) selected the EMG channel with the best artifact correction and/or most clear tremor activity(4). The other articles first Fourier transformed the EMG data, and selected EMG channel(s) based on the power spectra. Sharifi et al. (5) selected one channel with the highest distinct peak around the known tremor frequency, Broersma et al. (16) and Buijink et al. (15) averaged the three channels with the highest power to use for their analysis.

Secondly, a frequency band of interest was extracted from the power spectra of the selected channel(s). Richardson et al. (2) used the power spectrum between 6-30Hz, based on earlier research in patients with cortical tremor(17). Van Rootselaar et al. (3) extracted frequencies from 1 to 250 Hz, because this is generally the upper limit of significant EMG power(18). Contarino et al. (4) used this same frequency band of 1 to 250 Hz for the analysis of self-paced flexion-extension movement, but chose a narrower band around the tremor frequency for the analysis of the tremor evoking task. This method of selecting a frequency band around the tremor frequency was applied in the other articles too(5, 6, 11-16).

After the EMG channels and frequency band were selected, all articles calculated the average power in this range per time segment of the EMG-fMRI recording. The length of the segment was the same as the TR of the fMRI scan, to ensure that there was a EMG value in the EMG vector for every fMRI scan.

The next step in a part of the studies was to apply Gram-Schmidt orthogonalization with respect to the performed task (block), to make the EMG vectors and block-vectors independent(3-5, 15, 16). The other studies did not report orthogonalization of their data(2, 6, 11-14). However, the studies by Dirkx et al. (11-14) did perform another processing step on the EMG data. They calculated the first temporal derivative of the EMG-amplitude regressor (EMG-change), to capture activity related to changes in tremor amplitude.

Finally, all articles convolved their regressors with a hemodynamic response function, and used them as explanatory variables in a general linear model (GLM) (2-6, 11-16) About half of the articles, predominantly the more recently published, extended their analysis with a dynamic causal model (DCM) to investigate causal interactions between different brain areas (11-15).

An additional processing step some articles reported was normalization (5, 6, 11-14) or scaling (3, 15, 16) of their data. Five articles took the logarithmic value of the EMG data to remove outliers(2, 11-14).

Discussion

The aim this literature study was to systematically reviews current methods for a combined EMG-fMRI analysis in patients with tremor of the upper limb.

Action vs. rest tremor

In the included literature, the two most common diagnoses were essential tremor and tremor dominant Parkinson's Disease. Essential tremor patients typically suffer from postural tremor, which presents with maintenance of a particular posture, such as holding the arms outstretched in front of the body. (19) Postural tremor is a subclassification of action tremor, which occur with voluntary contraction of muscles. The patients in the studies by Richardson et al. (2) and Van Rootselaar et al. (3), who were diagnosed with familial cortical tremor and FCMTE respectively, suffered from action tremor too. Contrarily, tremor-dominant Parkinson's disease is characterized by rest tremor, which is present when the affected body part is not actively contracting and is supported against gravity(19).

This division between action and rest tremor was apparent in the study design of the included articles. Whereas the EMG-fMRI in studies about rest tremor was recorded while the participants were in rest, the participants in studies with action tremor were recorded while performing motor tasks. This was typically a posture task, evoking tremor in the patients, alternated with rest. Often, additionally self-paced wrist flexion-extension was performed. This resulted in the controls mimicking a tremor, which allowed for better comparison of a tremor like movement between action tremor patients and healthy controls. The participants in the study by Helmich et al. (6) performed a motor imagery task instead of a movement, to focus on brain regions related to the planning of movement rather than the execution itself. Sharifi et al. (5) incorporated sensory input into their research in essential tremor and PD patients, by using a wrist manipulator to separately identify the efferent motor network and the afferent sensory network with external perturbations. In some of the studies with PD patients, participants were exposed to mental stress during a part of the experiment, which resulted in increased activity in the noradrenergic system (13, 14). The authors hypothesized that the noradrenergic system is involved in generating tremor in PD, and explored this by comparing tremor amplitude in rest and stress, in the later situation resulting in increased activity in the noradrenergic system.

EMG regression analysis

When processing the EMG data to be used as a regressor in the fMRI analysis, a difference in

approach was found between articles which orthogonalized their EMG data and studies that did not. This depended on the type of tremor and therefore study design too. Orthogonalization of the EMG data is performed to separate the tremor related movement from the total recorded movement, which consists of both tremor- and motor task related movement.(3) In the situation of co-occurrence of tremor and voluntary movement, such as an action tremor while performing a motor task, orthogonalization of the data is of importance. In case of measurements without a motor task, for example to research rest tremor in PD patients, orthogonalization of the EMG data is not a relevant step for the analysis.

Besides the orthogonalization of the EMG data, there were other differences in the analyses between the articles. Some articles additionally performed processing steps to remove outliers (take logarithmic values), change the distribution (normalization) of their data for the analysis, or scale the data to prevent a particular measurement from dominating the results.

Once the EMG regressors had been prepared, they were fit to a general linear model, and around half of the articles secondarily extended their analysis with a dynamic causal model. In the GLMs, each voxel of the fMRI scans was tested to determine if there was, or was not, neural activity at a specific moment in time of the recording. (20) By adding EMG data of the tremor movement to the model as a regressor, this information could be used to identify brain regions with activity related to the tremor movement.(3) The added value of the DCM, is that information on the rate of change (= dynamics) in neural activity in response to incoming signals is used for the model. These incoming signals can be either from other brain regions, or 'new' exogeneous input from e.g. muscle activity. Because of this, causal interactions between brain regions and exogeneous input can be modeled, which can give more insight into how information propagates through different areas within a brain network. (20)

Furthermore, the analyzed brain areas differed slightly among the articles, although these were predominantly focused around a particular network. Around half of the articles used a whole brain search to identify brain regions related to the performed task, and a majority of the studies (additionally) performed an analysis which focused on the regions within the cerebello-thalamo-cortical network, as they expected this brain activity to be related to the pathophysiology of tremor. A couple of articles narrowed their ROI down to a specific part of this network, while one article added the olivary nucleus as a ROI to the analysis (5).

Thesis

During my thesis, I will investigate a potential central pathophysiology of neuropathic tremor in CIDP patients. This tremor has been characterized as an action tremor, but sometimes patients suffer from a resting tremor too. (9, 10) As this literature review has shown, a study design in which CIDP patients perform motor tasks to evoke tremor, would be suitable. This is in line with the already written study protocol.

The analysis steps to add the EMG data as a regressor to the fMRI analysis, have not been determined yet. In order to design this, the results of this literature review will be combined with characteristics of the recorded data. For example, the method for selecting channel(s) will partly depend on how effective artifact correction has been and how clearly tremor peaks are present in the pre-processed data. Likewise, the need for any additional steps to remove outliers, or normalize or scale the data to change the distribution for the analysis, will depend om the recorded data too. This literature review provides a number of options to consider for further processing of the data.

A relevant finding for my thesis in this literature review, is to orthogonalize your data in case of co-occurring tremor and movement from a performed motor task. Since CIDP patients predominantly suffer from action tremor, and during the experiment they will perform tremor evoking motor tasks, orthogonalization of the data will have to be applied to separate the tremor component in the EMG

data from the total recorded EMG data. Subsequently, the tremor related EMG data will be used as a regressor in the fMRI analysis.
An important point for my thesis is what network I hypothesize to be evolved in the pathophysiology of tremor in CIDP patients, and which brain areas will therefore be analyzed. The question about which brain networks are involved in voluntary movements, and how this might be altered in CIDP patients, was outside the scope of this literature review. Nevertheless, the included studies suggest that the cerebello-thalamo-cortical network might be involved. However, these studies were performed in patients with diagnosis different from CIDP, so during my thesis I will more extensively research which networks may be involved in tremor in CIDP.
If I have a hypothesis about a potential tremor network, I will start the analysis with a GLM to see if brain areas related to tremor can be detected in these patients. If this goes well, the analysis might be extended with a DCM.

Limitations and further research

This literature study focused on the methods of using EMG data as a regressor in fMRI analyses, which meant that a number of aspects received less attention. First of all, the results of the used methods were not taken into consideration. If these had been included, the effectivity of reviewed EMG regression methods could have been discussed and used to choose a preferable EMG regression method. However, the EMG analysis steps taken in the included studies were notably similar within an investigated tremor type and study design, which means that comparing their results was less relevant. Whenever there would be more diversity in applied methods, a comparison of their effectivity would be an interesting addition to the literature study. In case the results of different analysis methods would be compared, a quality assessment of the included literature should be considered. In this literature review, no quality assessment was executed.
A factor which may have influenced the applied EMG regression methods but was not investigated, is more details on the data acquisition and artifact correction. These steps were performed prior to the EMG regression steps that were reviewed in this literature study. However, due to available Toolboxes for pre-processing EMG data recorded simultaneously with fMRI acquisition, there might have been little variation in these steps between the articles. Another limitation was that data was solely extracted from the main article, while the supplementary materials could have given more details on the applied method for EMG regression.

Conclusion

The aim this literature study was to systematically reviews current methods for a combined EMG-fMRI analysis in patients with tremor of the upper limb. All articles started with a choice of channel(s) based on artifact correction and presence of a tremor peak, followed by a choice of frequency band of interest which was often a window around the tremor frequency, and subsequently made power spectra of the data for the analysis. For the next step, a difference in approach was found. Whereas studies including motor tasks in patients with an action tremor orthogonalized their data with respect to the task, studies investigating rest tremor did not. Additionally, some articles took logarithmic values of the data or normalized or scaled them. Finally, all articles convolved their EMG regressors with a hemodynamic response function and used this in a general linear model analysis. In some studies, this analysis was extended with a dynamic causal model.

References

1. Bucher SF, Seelos KC, Dodel RC, Reiser M, Oertel WH. Activation mapping in essential tremor with functional magnetic resonance imaging. Ann Neurol. 1997;41(1):32-40.
2. Richardson MP, Grosse P, Allen PJ, Turner R, Brown P. BOLD correlates of EMG spectral density in cortical myoclonus: description of method and case report. Neuroimage. 2006;32(2):558-65.
3. van Rootselaar AF, Maurits NM, Renken R, Koelman JH, Hoogduin JM, Leenders KL, et al. Simultaneous EMG-functional MRI recordings can directly relate hyperkinetic movements to brain activity. Hum Brain Mapp. 2008;29(12):1430-41.
4. Contarino MF, Groot PF, van der Meer JN, Bour LJ, Speelman JD, Nederveen AJ, et al. Is there a role for combined EMG-fMRI in exploring the pathophysiology of essential tremor and improving functional neurosurgery? PLoS One. 2012;7(10):e46234.
5. Sharifi S, Luft F, de Boer L, Buijink AWG, Mugge W, Schouten AC, et al. Closing the loop: Novel quantitative fMRI approach for manipulation of the sensorimotor loop in tremor. Neuroimage. 2022;262:119554.
6. Helmich RC, Bloem BR, Toni I. Motor imagery evokes increased somatosensory activity in Parkinson's disease patients with tremor. Hum Brain Mapp. 2012;33(8):1763-79.
7. Latov N. Diagnosis and treatment of chronic acquired demyelinating polyneuropathies. Nat Rev Neurol. 2014;10(8):435-46.
8. Broers MC, Bunschoten C, Nieboer D, Lingsma HF, Jacobs BC. Incidence and Prevalence of Chronic Inflammatory Demyelinating Polyradiculoneuropathy: A Systematic Review and Meta-Analysis. Neuroepidemiology. 2019;52(3-4):161-72.
9. Devaux JJ, Miura Y, Fukami Y, Inoue T, Manso C, Belghazi M, et al. Neurofascin-155 IgG4 in chronic inflammatory demyelinating polyneuropathy. Neurology. 2016;86(9):800-7.
10. Querol L, Nogales-Gadea G, Rojas-Garcia R, Diaz-Manera J, Pardo J, Ortega-Moreno A, et al. Neurofascin IgG4 antibodies in CIDP associate with disabling tremor and poor response to IVIg. Neurology. 2014;82(10):879-86.
11. Dirkx MF, den Ouden H, Aarts E, Timmer M, Bloem BR, Toni I, et al. The Cerebral Network of Parkinson's Tremor: An Effective Connectivity fMRI Study. J Neurosci. 2016;36(19):5362-72.
12. Dirkx MF, den Ouden HE, Aarts E, Timmer MH, Bloem BR, Toni I, et al. Dopamine controls Parkinson's tremor by inhibiting the cerebellar thalamus. Brain. 2017;140(3):721-34.
13. Dirkx MF, Zach H, van Nuland A, Bloem BR, Toni I, Helmich RC. Cerebral differences between dopamine-resistant and dopamine-responsive Parkinson's tremor. Brain. 2019;142(10):3144-57.
14. Dirkx MF, Zach H, van Nuland AJ, Bloem BR, Toni I, Helmich RC. Cognitive load amplifies Parkinson's tremor through excitatory network influences onto the thalamus. Brain. 2020;143(5):1498-511.
15. Buijink AW, van der Stouwe AM, Broersma M, Sharifi S, Groot PF, Speelman JD, et al. Motor network disruption in essential tremor: a functional and effective connectivity study. Brain. 2015;138(Pt 10):2934-47.
16. Broersma M, van der Stouwe AMM, Buijink AWG, de Jong BM, Groot PFC, Speelman JD, et al. Bilateral cerebellar activation in unilaterally challenged essential tremor. Neuroimage Clin. 2016;11:1-9.
17. Grosse P, Guerrini R, Parmeggiani L, Bonanni P, Pogosyan A, Brown P. Abnormal corticomuscular and intermuscular coupling in high-frequency rhythmic myoclonus. Brain. 2003;126(Pt 2):326-42.
18. Basmajian JV, Luca CJd. Muscles Alive : their functions revealed by electromyography. [5th ed.] ed. Baltimore: Williams & Wilkins; 1985.
19. Ha AD, Jankovic J. An Introduction to Dyskinesia—The Clinical Spectrum. In: Brotchie J, Bezard E, Jenner P, editors. International Review of Neurobiology. 98: Academic Press; 2011. p. 1-29.
20. Kahan J, Foltynie T. Understanding DCM: Ten simple rules for the clinician. NeuroImage. 2013;83.

Appendix C: Available Data per Participant

Participant	EMG data				fMRI data			
	D1	D2	S1	S2	D1	D2	S1	S2
Tremor group								
T1	x	x	x	x	x	x	x	x
T2	x		x		x		x	
T3	x	x	x		x	x	x	
T4	x	x	x	x	x	x	x	x
T5	x	x	x	x	x	x	x	x
T6	x	x	x		x	x	x	
T7	x		x		x		x	
T8	x	x	x	x	x	x	x	x
T9	x	x	x	x	x	x	x	x
Tx*	x	x	x	x				
Control group								
C1	x	x	x	x	x	x	x	x
C2	x	x	x	x	x	x	x	x
C3	x	x	x	x	x	x	x	x
C4	x		x		x		x	
C5	x				x			
C6	x	x	x	x	x	x	x	x
C7	x	x	x	x	x	x	x	x
C8	x	x**	x	x	x	x	x	x
C9					x	x	x	x
C10	x	x	x	x	x	x	x	x
C11	x	x	x	x	x	x	x	x
C12	x	x	x	x	x	x	x	x

D1: Dynamic motor task run 1; D2: Dynamic motor task run 2; S1: Static motor task run 1; S2: Static motor task run 2; Tx: excluded due to no fMRI data; ** error in pre-processing, not included in GLM*
x indicates that data is available

Appendix D: Second-Level-Analysis uncorrected p < 0.001

D.1 Static motor task

D.1.1 Static task within tremor group

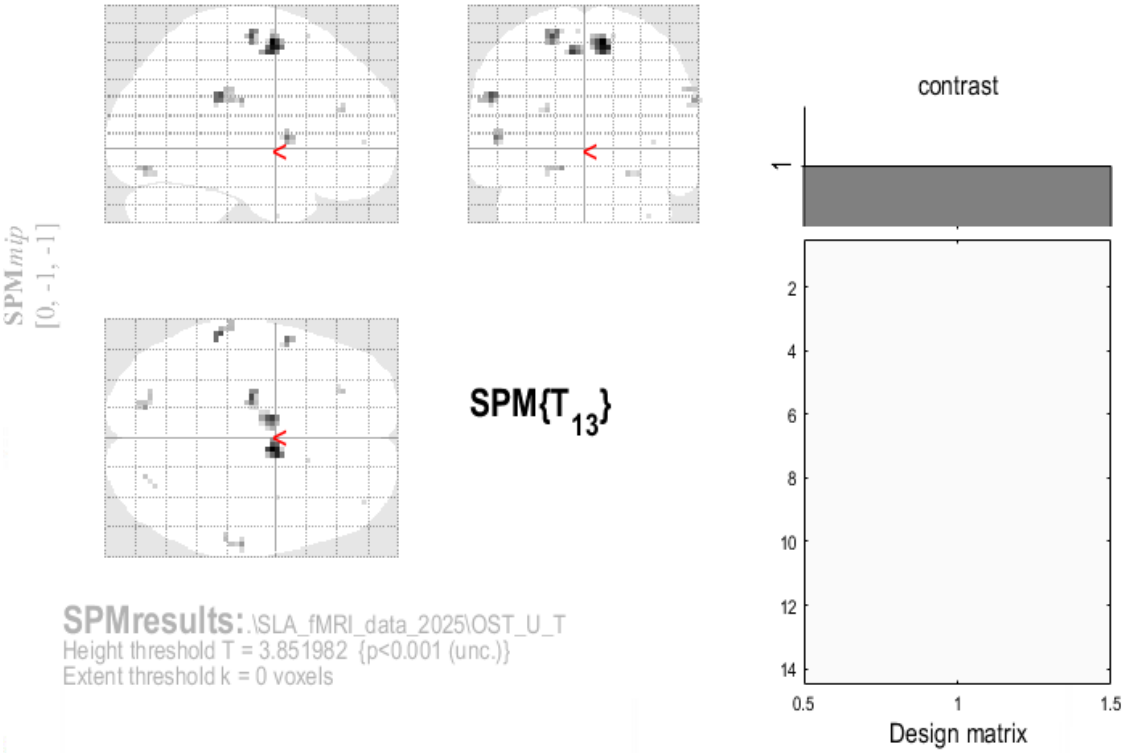

Statistics: ***p-values adjusted for search volume***

set-level		cluster-level				peak-level					mm mm mm		
p	c	$p_{FWE\text{-}corr}$	$q_{FDR\text{-}corr}$	k_E	p_{uncorr}	$p_{FWE\text{-}corr}$	$q_{FDR\text{-}corr}$	T	(Z_E)	p_{uncorr}			
0.095	14	0.193	0.319	32	0.023	0.430	0.709	6.23	4.17	0.000	9	-4	59
		0.478	0.391	19	0.069	0.704	0.709	5.56	3.91	0.000	-9	-4	53
		0.545	0.391	17	0.084	0.771	0.709	5.40	3.85	0.000	-21	-16	62
		0.654	0.396	14	0.113	0.791	0.709	5.35	3.82	0.000	-57	-34	29
		0.843	0.520	9	0.197	0.908	0.862	5.00	3.67	0.000	-54	5	5
		0.877	0.520	8	0.223	0.976	0.967	4.62	3.49	0.000	-15	-79	-13
		0.957	0.642	5	0.334	0.979	0.967	4.59	3.48	0.000	63	-22	26
		0.986	0.642	3	0.458	0.997	0.967	4.25	3.30	0.000	60	-31	32
		0.974	0.642	4	0.389	0.998	0.967	4.22	3.29	0.001	-24	38	20
		0.986	0.642	3	0.458	0.998	0.967	4.17	3.27	0.001	24	-79	-16
						1.000	0.967	3.98	3.16	0.001	30	-73	-16
		0.998	0.687	1	0.687	1.000	0.967	3.95	3.15	0.001	15	17	62
		0.998	0.687	1	0.687	1.000	0.967	3.92	3.13	0.001	-6	-4	65
		0.998	0.687	1	0.687	1.000	0.967	3.90	3.12	0.001	39	50	2
		0.998	0.687	1	0.687	1.000	0.967	3.88	3.11	0.001	36	-1	-40

D.1.2 Static task within control group

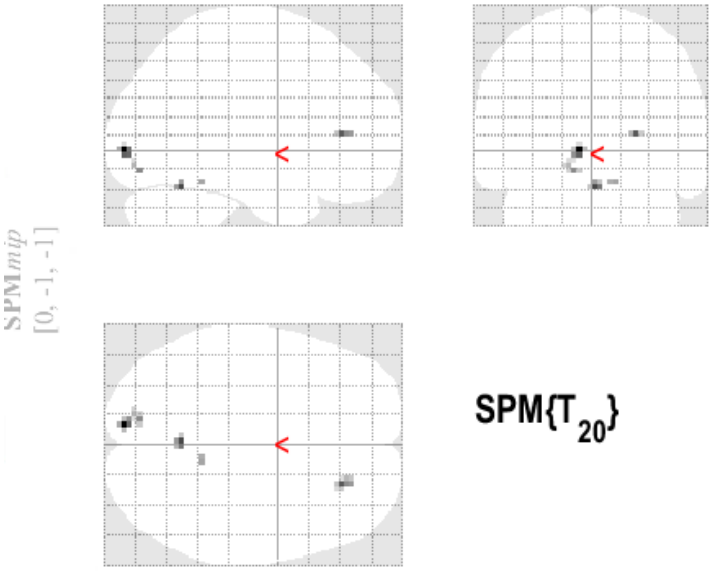

$SPM\{T_{20}\}$

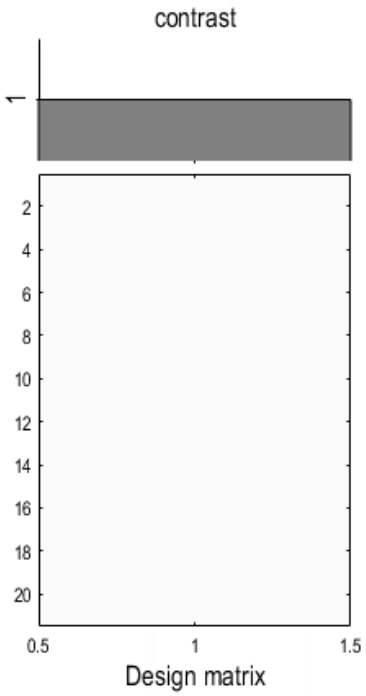

SPMresults: .\SLA_fMRI_data_2025\OST_U_NT
Height threshold T = 3.551808 {p<0.001 (unc.)}
Extent threshold k = 0 voxels

Statistics: ***p-values adjusted for search volume***

set-level		cluster-level				peak-level					mm mm mm
p	c	$p_{FWE\text{-}corr}$	$q_{FDR\text{-}corr}$	k_E	p_{uncorr}	$p_{FWE\text{-}corr}$	$q_{FDR\text{-}corr}$	T	(Z_E)	p_{uncorr}	
0.779	4	0.620	0.536	18	0.181	0.276	0.362	5.23	4.10	0.000	-9 -91 -1
						0.841	0.516	4.21	3.52	0.000	-12 -82 -13
		0.883	0.536	7	0.402	0.577	0.382	4.66	3.79	0.000	0 -58 -22
		0.838	0.536	9	0.341	0.639	0.382	4.56	3.73	0.000	24 35 8
		0.973	0.674	2	0.674	0.923	0.578	4.01	3.39	0.000	12 -46 -19

D.1.3 Comparison tremor and control group static task

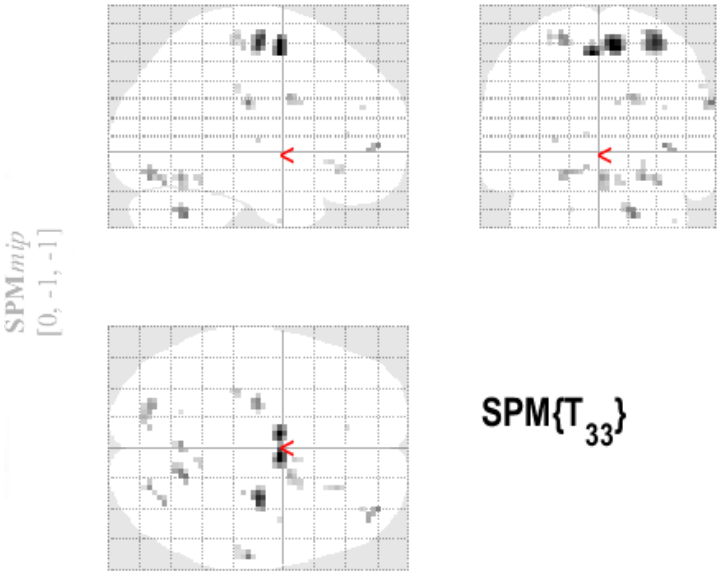

SPM{T_{33}}

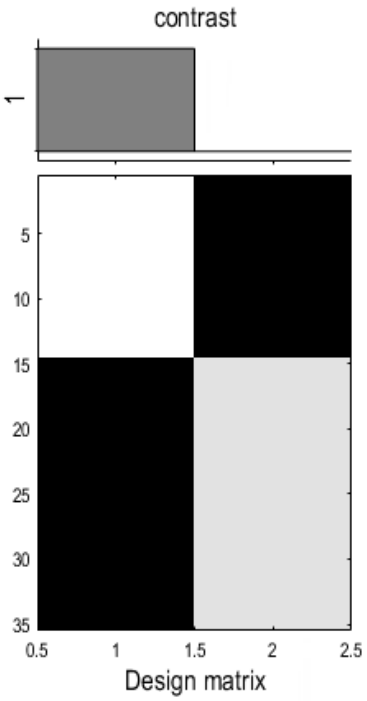

SPMresults: .\SLA_fMRI_data_2025\TST_U
Height threshold T = 3.356337 {p<0.001 (unc.)}
Extent threshold k = 0 voxels

Statistics: ***p-values adjusted for search volume***

set-level		cluster-level				peak-level					mm mm mm		
p	c	$p_{FWE\text{-}corr}$	$q_{FDR\text{-}corr}$	k_E	p_{uncorr}	$p_{FWE\text{-}corr}$	$q_{FDR\text{-}corr}$	T	(Z_E)	p_{uncorr}			
0.000	22	0.135	0.499	52	0.027	0.042	0.125	5.52	4.61	0.000	6	-4	56
						0.044	0.125	5.50	4.60	0.000	-6	-4	53
		0.219	0.499	41	0.045	0.114	0.222	5.10	4.35	0.000	30	-16	59
		0.751	0.771	12	0.256	0.479	0.694	4.38	3.86	0.000	18	-58	-37
		0.829	0.771	9	0.325	0.490	0.694	4.36	3.85	0.000	63	-22	26
		0.900	0.771	6	0.424	0.593	0.694	4.23	3.76	0.000	36	53	2
						0.830	0.731	3.92	3.53	0.000	42	47	-1
		0.725	0.771	13	0.237	0.634	0.694	4.18	3.72	0.000	-24	-16	62
		0.803	0.771	10	0.299	0.696	0.731	4.10	3.66	0.000	24	-79	-16
						0.805	0.731	3.96	3.55	0.000	33	-70	-19
		0.751	0.771	12	0.256	0.771	0.731	4.01	3.59	0.000	0	-61	-16
		0.751	0.771	12	0.256	0.778	0.731	4.00	3.58	0.000	-21	-79	-13
		0.751	0.771	12	0.256	0.844	0.731	3.90	3.51	0.000	18	2	29
		0.973	0.771	2	0.662	0.940	0.877	3.70	3.36	0.000	27	-25	56
		0.985	0.771	1	0.771	0.944	0.877	3.68	3.35	0.000	-9	-79	-10
		0.900	0.771	6	0.424	0.944	0.877	3.68	3.35	0.000	-30	-28	62
		0.900	0.771	6	0.424	0.951	0.877	3.66	3.33	0.000	24	29	-13
		0.973	0.771	2	0.662	0.971	0.919	3.58	3.27	0.001	9	5	26
		0.941	0.771	4	0.519	0.977	0.919	3.55	3.24	0.001	12	-49	-19
		0.985	0.771	1	0.771	0.977	0.919	3.55	3.24	0.001	-27	-16	5
		0.958	0.771	3	0.582	0.991	0.961	3.43	3.15	0.001	57	-28	35
		0.985	0.771	1	0.771	0.991	0.961	3.43	3.15	0.001	36	44	23
		0.985	0.771	1	0.771	0.993	0.961	3.40	3.12	0.001	42	-4	-40
		0.985	0.771	1	0.771	0.994	0.961	3.40	3.12	0.001	-9	35	8
		0.985	0.771	1	0.771	0.994	0.961	3.38	3.11	0.001	-18	-61	-34

D.2 Dynamic motor task

D.2.1 Dynamic task within tremor group

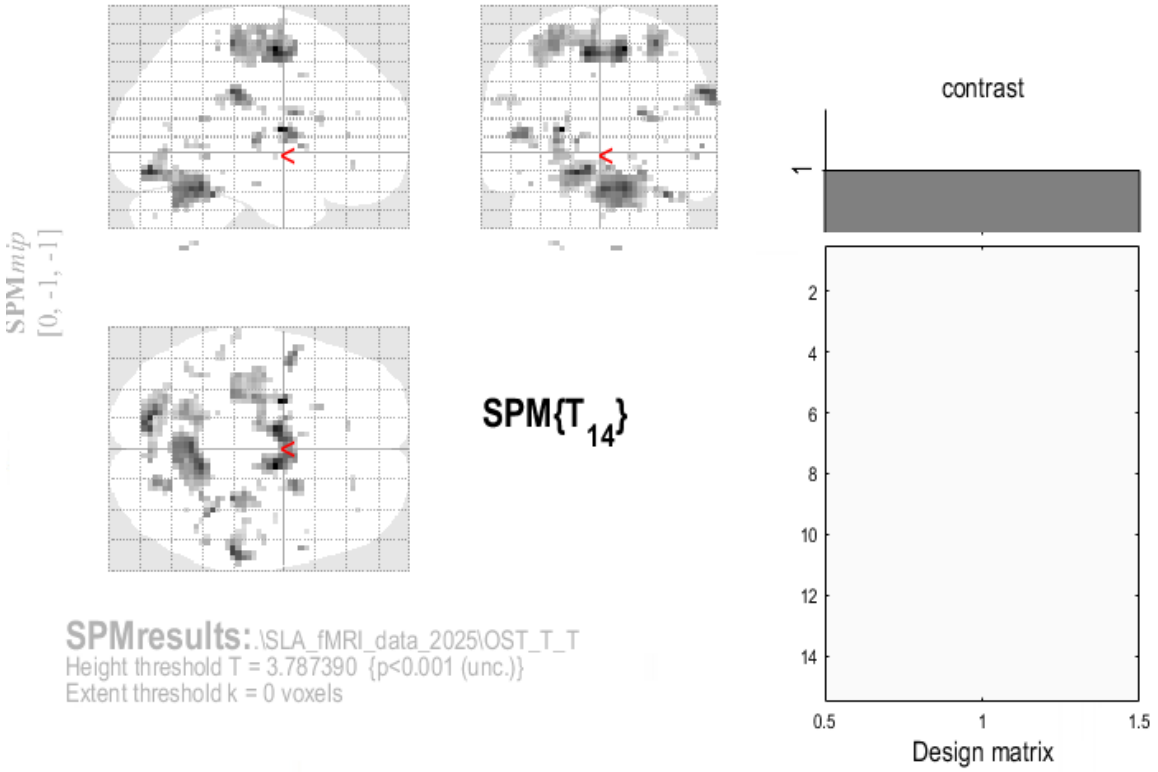

Statistics: ***p-values adjusted for search volume***

set-level		cluster-level				peak-level					mm mm mm		
p	*c*	$p_{FWE\text{-}corr}$	$q_{FDR\text{-}corr}$	k_E	p_{uncorr}	$p_{FWE\text{-}corr}$	$q_{FDR\text{-}corr}$	*T*	(Z_E)	p_{uncorr}			
0.000	40	0.786	0.720	11	0.196	0.073	0.399	7.47	4.67	0.000	-24	-4	11
		0.000	0.000	385	0.000	0.081	0.399	7.40	4.65	0.000	12	-7	56
						0.138	0.424	6.95	4.50	0.000	-9	-7	53
						0.676	0.571	5.30	3.86	0.000	-30	-31	59
		0.000	0.000	399	0.000	0.193	0.424	6.64	4.39	0.000	-15	-79	-13
						0.258	0.424	6.37	4.29	0.000	12	-49	-22
						0.299	0.424	6.23	4.24	0.000	0	-55	-22
		0.065	0.086	55	0.009	0.287	0.424	6.26	4.26	0.000	60	-31	32
						0.992	0.781	4.18	3.31	0.000	42	-25	23
		0.034	0.059	67	0.004	0.370	0.432	6.01	4.16	0.000	30	-31	59
		0.654	0.676	15	0.135	0.380	0.432	5.99	4.15	0.000	36	-43	-25
						0.972	0.734	4.41	3.43	0.000	45	-52	-25
		0.422	0.545	23	0.070	0.550	0.571	5.58	3.98	0.000	-51	5	8
		0.622	0.676	16	0.124	0.586	0.571	5.50	3.95	0.000	21	5	20
		0.753	0.720	12	0.178	0.637	0.571	5.39	3.90	0.000	-27	-19	5
		0.968	0.720	4	0.436	0.703	0.571	5.25	3.84	0.000	-15	-1	5
		0.474	0.545	21	0.082	0.722	0.571	5.21	3.82	0.000	21	-76	-13
						0.805	0.571	5.01	3.73	0.000	24	-67	-13
		0.991	0.720	2	0.593	0.846	0.571	4.91	3.68	0.000	57	8	2
		0.950	0.720	5	0.382	0.849	0.571	4.90	3.68	0.000	27	-49	17
		0.981	0.720	3	0.504	0.934	0.629	4.62	3.54	0.000	6	-61	-55

Statistics: ***p-values adjusted for search volume***

set-level		cluster-level				peak-level					mm mm mm		
p	c	$p_{FWE\text{-}corr}$	$q_{FDR\text{-}corr}$	k_E	p_{uncorr}	$p_{FWE\text{-}corr}$	$q_{FDR\text{-}corr}$	T	(Z_E)	p_{uncorr}			
		0.991	0.720	2	0.593	0.935	0.629	4.62	3.54	0.000	33	-40	56
		0.981	0.720	3	0.504	0.938	0.629	4.60	3.53	0.000	54	-46	-4
		0.849	0.720	9	0.241	0.953	0.667	4.53	3.50	0.000	-39	-49	2
						0.987	0.759	4.25	3.35	0.000	-42	-58	2
		0.950	0.720	5	0.382	0.955	0.667	4.52	3.49	0.000	-21	20	17
		0.991	0.720	2	0.593	0.962	0.687	4.48	3.47	0.000	-42	-16	-19
		0.991	0.720	2	0.593	0.980	0.757	4.33	3.39	0.000	-12	35	8
		0.950	0.720	5	0.382	0.986	0.759	4.27	3.36	0.000	51	-13	23
		0.981	0.720	3	0.504	0.987	0.759	4.26	3.35	0.000	24	38	-7
		0.991	0.720	2	0.593	0.987	0.759	4.26	3.35	0.000	-27	-52	-52
		0.991	0.720	2	0.593	0.988	0.760	4.24	3.34	0.000	-6	8	41
		0.878	0.720	8	0.268	0.992	0.781	4.18	3.31	0.000	-54	-37	26
		0.991	0.720	2	0.593	0.993	0.781	4.16	3.30	0.000	21	-16	56
		0.991	0.720	2	0.593	0.996	0.860	4.06	3.25	0.001	-15	-16	2
		0.996	0.720	1	0.720	0.997	0.860	4.04	3.24	0.001	-18	-40	65
		0.929	0.720	6	0.337	0.997	0.860	4.04	3.23	0.001	-60	-28	26
		0.996	0.720	1	0.720	0.997	0.860	4.03	3.23	0.001	24	-13	20
		0.981	0.720	3	0.504	0.998	0.875	4.00	3.21	0.001	-33	-67	11
		0.996	0.720	1	0.720	0.998	0.884	3.98	3.20	0.001	-48	-37	-13
		0.996	0.720	1	0.720	0.998	0.884	3.97	3.19	0.001	30	-37	23
		0.996	0.720	1	0.720	0.998	0.884	3.95	3.18	0.001	0	-76	-37
		0.991	0.720	2	0.593	0.999	0.884	3.94	3.18	0.001	15	-7	-4
		0.996	0.720	1	0.720	0.999	0.884	3.93	3.17	0.001	-24	-58	-55
		0.996	0.720	1	0.720	0.999	0.901	3.91	3.16	0.001	36	-58	5
		0.996	0.720	1	0.720	0.999	0.904	3.89	3.15	0.001	36	41	20
		0.991	0.720	2	0.593	0.999	0.926	3.86	3.13	0.001	39	-7	53
		0.996	0.720	1	0.720	0.999	0.943	3.83	3.12	0.001	48	11	-1

D.2.2 Dynamic task within control group

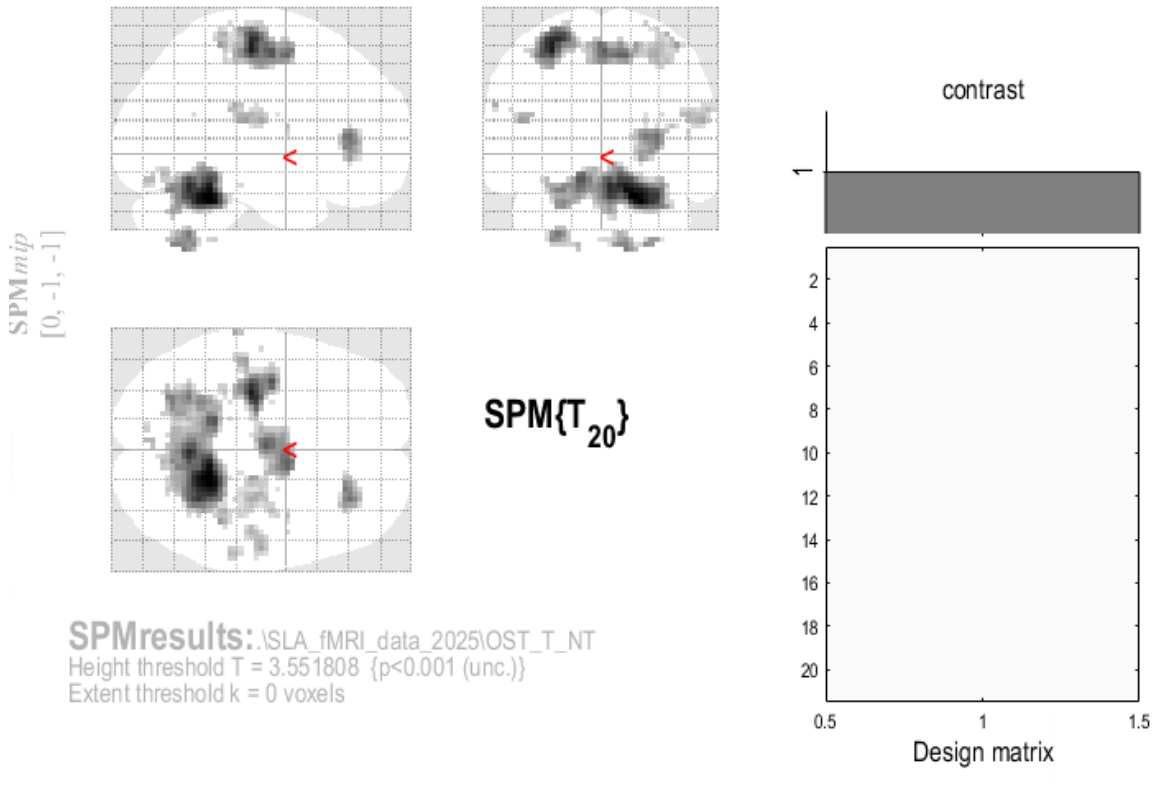

Statistics: ***p-values adjusted for search volume***

set-level		cluster-level				peak-level					mm mm mm		
p	c	$p_{FWE\text{-}corr}$	$q_{FDR\text{-}corr}$	k_E	p_{uncorr}	$p_{FWE\text{-}corr}$	$q_{FDR\text{-}corr}$	T	(Z_E)	p_{uncorr}			
0.000	28	0.000	0.000	973	0.000	0.020	0.251	6.72	4.80	0.000	18	-46	-25
						0.066	0.279	6.01	4.49	0.000	3	-58	-19
						0.170	0.441	5.43	4.21	0.000	-12	-43	-16
		0.000	0.000	618	0.000	0.046	0.279	6.22	4.59	0.000	-30	-22	56
						0.164	0.441	5.45	4.22	0.000	-36	-10	56
						0.198	0.441	5.33	4.16	0.000	0	-13	56
		0.035	0.075	102	0.008	0.280	0.493	5.10	4.04	0.000	30	35	8
						0.621	0.624	4.47	3.68	0.000	21	35	-4
		0.166	0.263	55	0.041	0.346	0.493	4.95	3.96	0.000	-27	-58	-46
						0.832	0.780	4.11	3.46	0.000	-15	-58	-52
		0.191	0.263	51	0.048	0.383	0.493	4.88	3.91	0.000	12	-61	-55
						0.485	0.580	4.70	3.81	0.000	24	-55	-52
		0.620	0.802	18	0.220	0.628	0.624	4.46	3.67	0.000	-48	-25	17
		0.220	0.263	47	0.056	0.712	0.715	4.33	3.59	0.000	57	-16	17
						0.787	0.757	4.20	3.51	0.000	48	-22	20
		0.938	0.802	3	0.632	0.723	0.715	4.31	3.58	0.000	-63	-31	26
		0.901	0.802	5	0.524	0.810	0.780	4.16	3.49	0.000	-3	-79	-16
		0.839	0.802	8	0.414	0.831	0.780	4.12	3.46	0.000	9	-73	-13
		0.795	0.802	10	0.359	0.853	0.803	4.07	3.43	0.000	60	-34	23
		0.938	0.802	3	0.632	0.870	0.803	4.03	3.41	0.000	39	-1	14
		0.955	0.802	2	0.704	0.924	0.914	3.89	3.32	0.000	-30	-37	-25
		0.920	0.802	4	0.573	0.934	0.914	3.86	3.30	0.000	6	-43	-49
		0.971	0.802	1	0.802	0.945	0.914	3.82	3.27	0.001	24	-16	71
		0.901	0.802	5	0.524	0.949	0.914	3.80	3.26	0.001	-33	-40	65
		0.920	0.802	4	0.573	0.955	0.914	3.78	3.24	0.001	-9	-82	-19
		0.955	0.802	2	0.704	0.957	0.914	3.77	3.24	0.001	30	-31	68
		0.955	0.802	2	0.704	0.958	0.914	3.76	3.23	0.001	48	-1	11
		0.971	0.802	1	0.802	0.969	0.924	3.70	3.19	0.001	-54	-16	23
		0.938	0.802	3	0.632	0.975	0.950	3.66	3.17	0.001	24	-16	17
		0.955	0.802	2	0.704	0.977	0.950	3.65	3.16	0.001	60	-19	26
		0.971	0.802	1	0.802	0.980	0.950	3.63	3.15	0.001	15	-28	-19
		0.971	0.802	1	0.802	0.982	0.950	3.62	3.13	0.001	33	-55	20
		0.971	0.802	1	0.802	0.982	0.950	3.61	3.13	0.001	-15	-34	-25
		0.971	0.802	1	0.802	0.983	0.950	3.61	3.13	0.001	-24	-34	71
		0.971	0.802	1	0.802	0.985	0.950	3.59	3.11	0.001	24	-7	20
		0.971	0.802	1	0.802	0.985	0.950	3.59	3.11	0.001	-24	-10	56

D.2.3 Comparison tremor and control group dynamic task

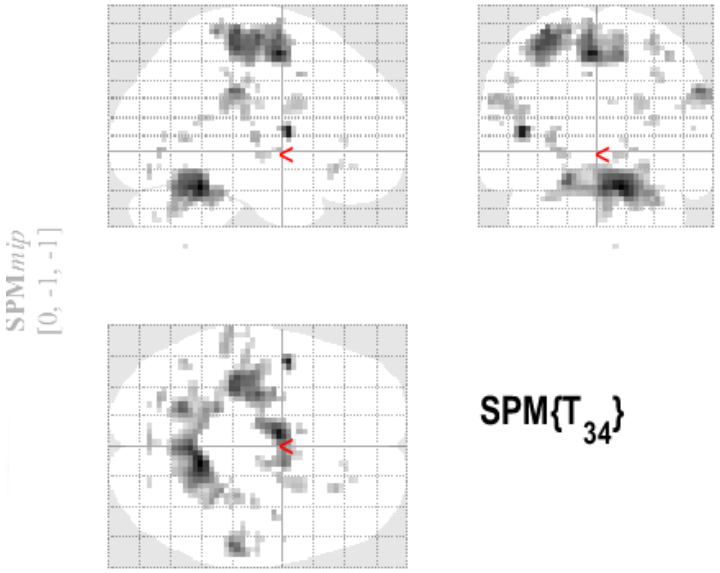

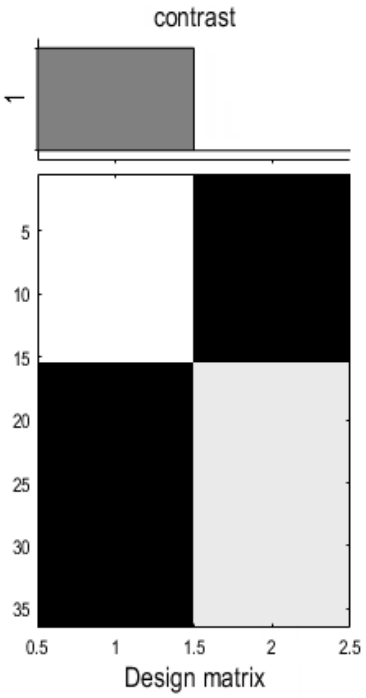

SPMresults: .\SLA_fMRI_data_2025\TST_T
Height threshold T = 3.347934 {p<0.001 (unc.)}
Extent threshold k = 0 voxels

Statistics: ***p-values adjusted for search volume***

set-level		cluster-level				peak-level					mm mm mm		
p	c	$p_{FWE\text{-}corr}$	$q_{FDR\text{-}corr}$	k_E	p_{uncorr}	$p_{FWE\text{-}corr}$	$q_{FDR\text{-}corr}$	T	(Z_E)	p_{uncorr}			
0.000	36	0.000	0.000	526	0.000	0.002	0.030	6.60	5.26	0.000	12	-49	-22
						0.019	0.063	5.75	4.77	0.000	3	-55	-22
						0.068	0.110	5.22	4.44	0.000	-18	-61	-19
		0.000	0.000	553	0.000	0.006	0.034	6.20	5.04	0.000	-6	-4	53
						0.038	0.091	5.46	4.60	0.000	-36	-28	56
						0.040	0.091	5.44	4.58	0.000	-30	-28	65
		0.485	0.792	24	0.144	0.008	0.034	6.12	4.99	0.000	-45	2	8
		0.091	0.248	68	0.021	0.083	0.116	5.13	4.39	0.000	57	-31	32
						0.938	0.769	3.61	3.29	0.000	54	-16	26
		0.261	0.591	40	0.066	0.567	0.429	4.17	3.72	0.000	-63	-31	26
						0.609	0.429	4.12	3.68	0.000	-54	-34	26
		0.673	0.792	15	0.243	0.568	0.429	4.17	3.72	0.000	30	-28	59
		0.837	0.792	8	0.394	0.602	0.429	4.13	3.69	0.000	-24	-73	-1
		0.814	0.792	9	0.365	0.603	0.429	4.13	3.69	0.000	-30	-16	5
		0.903	0.792	5	0.506	0.605	0.429	4.12	3.69	0.000	39	-7	53
		0.941	0.792	3	0.616	0.666	0.485	4.05	3.63	0.000	-6	8	41
		0.719	0.792	13	0.276	0.685	0.485	4.02	3.61	0.000	27	29	-10
		0.767	0.792	11	0.316	0.696	0.485	4.01	3.60	0.000	0	-79	-13
		0.628	0.792	17	0.215	0.701	0.485	4.00	3.60	0.000	-45	-25	20
		0.860	0.792	7	0.427	0.719	0.495	3.98	3.58	0.000	-45	-58	5
		0.814	0.792	9	0.365	0.750	0.525	3.94	3.55	0.000	-51	-22	38

Statistics: ***p-values adjusted for search volume***

set-level		cluster-level				peak-level					mm mm mm		
p	c	$p_{FWE\text{-}corr}$	$q_{FDR\text{-}corr}$	k_E	p_{uncorr}	$p_{FWE\text{-}corr}$	$q_{FDR\text{-}corr}$	T	(Z_E)	p_{uncorr}			
		0.860	0.792	7	0.427	0.790	0.566	3.88	3.51	0.000	33	-19	56
		0.941	0.792	3	0.616	0.803	0.566	3.87	3.50	0.000	21	-4	-1
		0.941	0.792	3	0.616	0.819	0.568	3.84	3.48	0.000	-24	-4	11
		0.330	0.626	34	0.087	0.820	0.568	3.84	3.48	0.000	24	8	26
		0.814	0.792	9	0.365	0.843	0.598	3.81	3.45	0.000	30	-34	41
		0.860	0.792	7	0.427	0.869	0.641	3.76	3.41	0.000	9	-16	-4
		0.923	0.792	4	0.556	0.908	0.736	3.68	3.35	0.000	60	-16	35
		0.837	0.792	8	0.394	0.925	0.761	3.64	3.32	0.000	30	-52	14
		0.974	0.792	1	0.792	0.932	0.769	3.62	3.31	0.000	54	-1	11
		0.941	0.792	3	0.616	0.944	0.778	3.59	3.28	0.001	6	5	26
		0.974	0.792	1	0.792	0.951	0.789	3.57	3.26	0.001	21	-31	-28
		0.941	0.792	3	0.616	0.952	0.789	3.56	3.26	0.001	-60	-22	17
		0.974	0.792	1	0.792	0.956	0.792	3.55	3.25	0.001	-57	-19	14
		0.923	0.792	4	0.556	0.958	0.792	3.54	3.24	0.001	15	35	5
		0.958	0.792	2	0.691	0.962	0.792	3.53	3.23	0.001	-30	-70	8
		0.958	0.792	2	0.691	0.963	0.792	3.52	3.23	0.001	24	-79	-13
		0.974	0.792	1	0.792	0.972	0.839	3.48	3.20	0.001	-21	-79	-13
		0.958	0.792	2	0.691	0.973	0.839	3.48	3.19	0.001	21	38	-10
		0.941	0.792	3	0.616	0.975	0.842	3.46	3.18	0.001	0	-76	-37
		0.974	0.792	1	0.792	0.977	0.845	3.45	3.17	0.001	9	-58	-55
		0.974	0.792	1	0.792	0.985	0.922	3.40	3.13	0.001	-21	-73	-10